UNIVERSIDADE FEDERAL DO PARANÁ

AMANDA GEROTTO

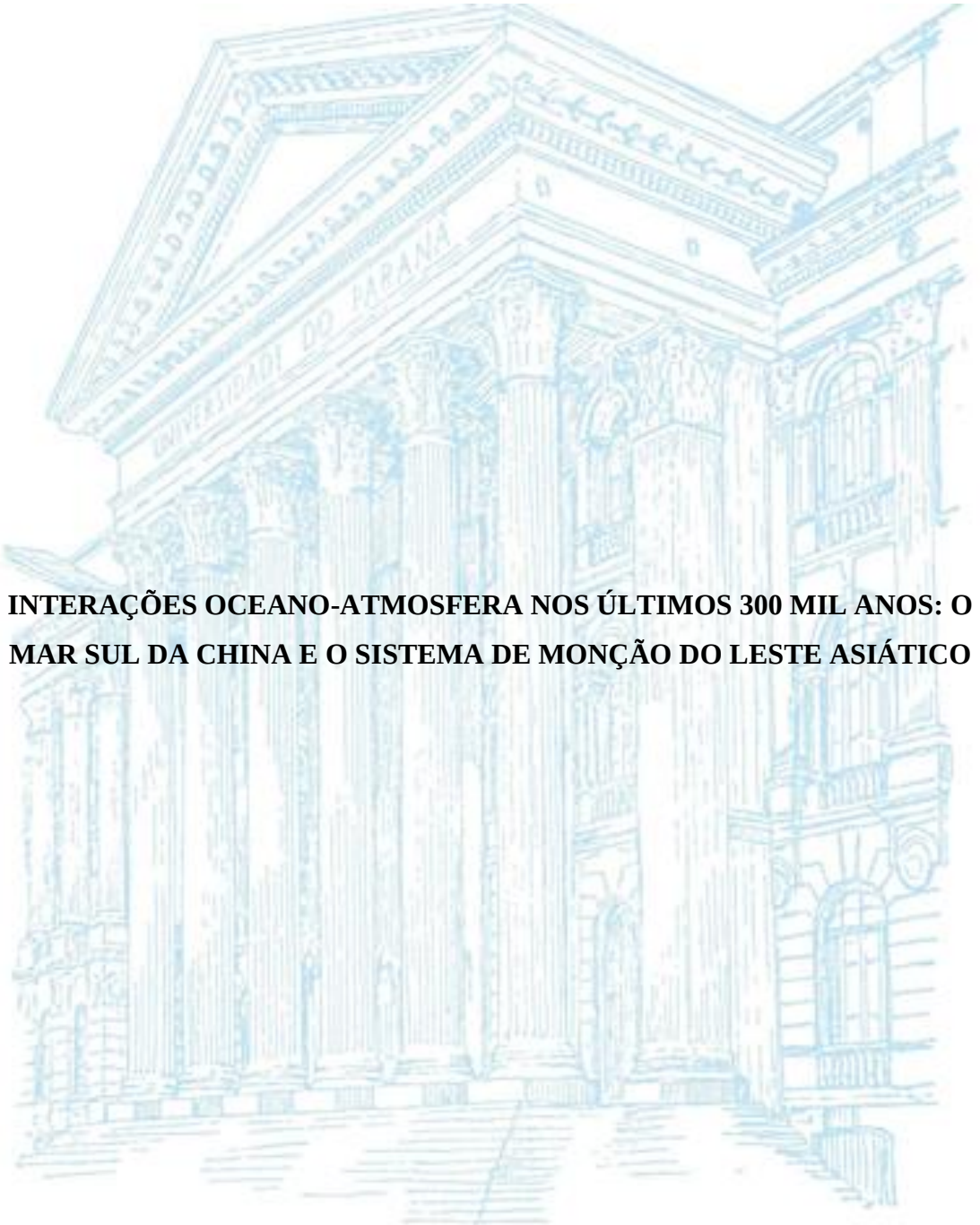

INTERAÇÕES OCEANO-ATMOSFERA NOS ÚLTIMOS 300 MIL ANOS: O MAR SUL DA CHINA E O SISTEMA DE MONÇÃO DO LESTE ASIÁTICO

PONTAL DO PARANÁ

2017

AMANDA GEROTTO

INTERAÇÕES OCEANO-ATMOSFERA NOS ÚLTIMOS 300 MIL ANOS: O MAR SUL DA CHINA E O SISTEMA DE MONÇÃO DO LESTE ASIÁTICO

Dissertação apresentada ao Curso de Mestrado em Sistemas Costeiros e Oceânicos, Setor de Ciências da Terra da Universidade Federal do Paraná, como requisito parcial para obtenção do título de Mestre. Área de concentração: Dinâmica Costeira e Oceânica.

Orientadora: Dra. Renata Hanae Nagai

PONTAL DO PARANÁ

2017

MINISTÉRIO DA EDUCAÇÃO
UNIVERSIDADE FEDERAL DO PARANÁ
PRÓ-REITORIA DE PESQUISA E PÓS-GRADUAÇÃO
Setor CIÊNCIAS DA TERRA
Programa de Pós-Graduação SISTEMAS COSTEIROS E OCEÂNICOS

TERMO DE APROVAÇÃO

Os membros da Banca Examinadora designada pelo Colegiado do Programa de Pós-Graduação em SISTEMAS COSTEIROS E OCEÂNICOS da Universidade Federal do Paraná foram convocados para realizar a arguição da dissertação de Mestrado de **AMANDA GEROTTO** intitulada: **Interações oceano-atmosfera nos últimos 300 mil anos: o Mar Sul da China e o Sistema de Monção do Leste Asiático**, após terem inquirido a aluna e realizado a avaliação do trabalho, são de parecer pela sua aprovação no rito de defesa.

A outorga do título de mestre está sujeita à homologação pelo colegiado, ao atendimento de todas as indicações e correções solicitadas pela banca e ao pleno atendimento das demandas regimentais do Programa de Pós-Graduação.

Pontal do Paraná, 23 de Maio de 2017.

RENATA HANAE NAGAI
Presidente da Banca Examinadora (UFPR)

RODRIGO PORTILHO RAMOS
Avaliador Externo (USP)

CÉSAR DE CASTRO MARTINS
Avaliador Interno (UFPR)

Dedicado ao meu sobrinho Davi Gerotto Melo, que sempre reascende minha esperança no futuro.

AGRADECIMENTOS

Agradeço primeiramente às oportunidades que me permitiram, não sem esforço, cursar a pós-graduação. Boa parte desse caminho foi proporcionada pelo esforço e amor da minha família, em especial minha mãe Maria Selma Firmino Gerotto e meu pai Waldemar Gerotto, minha irmã Aline Gerotto Melo, e minha tia Rita Aparecida Firmino.

Agradeço à minha orientadora Prof. Dra. Renata Hanae Nagai, pelos ensinamentos (Prof., você é um ponto fora da curva!) e inspiração. Foi durante esse trabalho e sob essa supervisão que definitivamente me vi na ciência e querendo fazer parte disso.

Durante o mestrado, e esses dois anos em Pontal do Sul, muitas pessoas contribuíram para que esse caminho fosse tão melhor que chegar. Melina Chiba Galvão, Ana Carolina Villas-Boas, Geórgia Aragão, obrigada por compartilharem os primeiros meses e os melhores cafés da manhã no Chalé; Thayanne Lima e Arian Larroque, obrigada por compartilharem essa mesma moradia comigo, e os pães/lanches no final da tarde. Vocês todos e o Chalé me acolheram e me ensinaram muito, e compartilharam os melhores momentos que vivi durante essa jornada. Obrigada! Guilherme Tebet e Giggia Barreto, obrigada pelas conversas que sempre clareiam minhas ideias, pelas caronas de bike (Gui) e por sempre estarem presentes comigo em Pontal!

Agradeço a presença, mesmo distante, de pessoas que são fundamentais no meu crescimento, meus amigos amados Kaique Francisco Silva, Paulo Mantoan, Gabriel Ayres, Maria Eduarda Laranjeira, Lauryne Alves e Fernanda Custódio (Ozzy). Vocês foram fundamentais na minha escolha em seguir essa jornada.

Agradeço aos caminhos que me fizeram chegar até Pontal do Sul, onde conheci tantas pessoas e uma fauna maravilhosa!

Minha permanência na pós-graduação só foi possível graças à bolsa concedida pela CAPES (Coordenação de Aperfeiçoamento de Pessoal de Nível Superior). Agradeço aos programas de auxílio e incentivo a pesquisa que permitem a realização desses trabalhos. As amostras do registro U1431D provêm do *International Ocean Discovery Program* (IODP), com auxílio IODP/CAPES-Brasil (Edital 38/2014) e FAPESP (Proc. n°2015/11832-2).

“If you assume that there is no hope, you guarantee that there will be no hope. If you assume that there is an instinct for freedom, that there are opportunities to change things, then there is a possibility that you can contribute to making a better world.”

(Captain Fantastic, Matt Ross, 2016)

RESUMO

A evolução dos padrões oceanográficos e climáticos do nosso planeta está diretamente ligada à alternância de ciclos glaciais e interglaciais que ocorreram durante o Quaternário associados à diversos atores da regulação climática. Os oceanos tropicais, como o Mar Sul da China (SCS), têm papel fundamental dentro desses processos, como uma importante região de comunicação entre altas e baixas latitudes. Analogamente, na atmosfera, o Sistema de Monção do Leste Asiático (EAM), permite esta comunicação. O EAM influencia significativamente os padrões oceanográficos sazonais do SCS, e suas interações estão intimamente ligados aos principais eventos climáticos registrados no Quaternário Superior. A presente dissertação investigou mudanças nas interações oceano-atmosfera entre o SCS e o EAM através de foraminíferos planctônicos de registros sedimentares marinhos, uma vez que este *proxy* permite inferir mudanças na estrutura da coluna d'água, no que diz respeito à produtividade primária e temperatura. A porcentagem de foraminíferos subsuperficiais/termoclina obtida em 11 registros sedimentares marinhos permitiu avaliar a variação espacial e temporal da camada de mistura (MLD) do SCS nos últimos 25 mil anos. Nesse período, variações da MLD estão relacionadas a variações na intensidade do EAM de inverno, em resposta a teleconecções atmosféricas de alta e baixas latitudes. A caracterização das assembleias de foraminíferos planctônicos do testemunho U1431D, retirado da região de mar profundo da porção leste do SCS durante o *International Ocean Discovery Program* (IODP) *Expedition* 349, foi aplicada no entendimento das condições ambientais (temperatura da superfície do mar e produtividade primária) no SCS nos últimos 300 mil anos. A evolução dos padrões hidrográficos do SCS apresenta forte relação com a mudanças na intensidade do EAM, especialmente nos eventos glaciais mais recentes. Nossos resultados apontam para a existência de gradientes latitudinais e longitudinais no SCS em resposta ao EAM e a entrada de águas do Pacífico, pela Corrente de Kuroshio.

Palavras-chave: Interações oceano-atmosfera; Mar Sul da China; Sistema de Monção do Leste Asiático; Foraminíferos planctônicos; Quaternário Superior.

ABSTRACT

Earth's oceanographic and climatic evolution is directly linked to Quaternary glacial and interglacial cycles driven by multiple climate regulation actors. Tropical oceans, as the South China Sea (SCS), play a key role in these processes as an important region of communication between high and low latitudes. Analogous, in the atmosphere, the East Asian Monsoon system (EAM) allows this communication. The EAM significantly influences the seasonal oceanographic patterns of the SCS, and the air-sea coupling between them are closely related to the major glacial/interglacial events recorded in the Late Quaternary. The present dissertation investigated changes in these air-sea interactions by examining planktonic foraminifera (PF) from marine sedimentary records, as this proxy allows the inference of water column conditions, particularly concerning primary productivity (PP) and upper thermal structure. The percentage of deep-dwellers PF obtained in 11 marine sedimentary records allowed to evaluate the spatial and temporal variation of the SCS mixed layer depth (MLD) in the last 25 thousand years. During this period, MLD variations are related to variations in EAM winter intensity in response to atmospheric teleconnections between high and low latitudes. The planktonic foraminifera assemblages from hole U1431D, taken from deep sea floor in the eastern SCS portion during the International Ocean Discovery Program (IODP) Expedition 349, was applied in understanding the SCS environmental conditions (sea surface temperature and primary productivity) in the last 300 thousand years. The SCS hydrographic patterns evolution is strongly related to EAM intensity changes, especially in recent cold events. Our results point to the existence of latitudinal and longitudinal gradients in SCS in response to EAM and the intrusion of Pacific waters by the Kuroshio Current.

Key-words: Ocean-atmosphere interactions; South China Sea; East Asian Monsoon System; Planktonic Foraminifera; Late Quaternary.

SUMÁRIO

INTRODUÇÃO

A evolução do clima no Quaternário Superior é marcada por ciclos glaciais e interglaciais decorrentes de mudanças nos padrões orbitais da Terra que afetaram os padrões climáticos e oceanográficos do nosso planeta (CLEMENS et al., 2010). Estas mudanças estão relacionadas com a interação de diversos atores da regulação climática, tais como: intensidade de insolação, circulação oceânica e atmosférica, mecanismos de *feedback* internos promovidos pela concentração de CO_2 atmosférico, intensidade do albedo, resfriamento de águas profundas e mudanças na profundidade da camada de mistura (LANG; WOLFF, 2011; MCCLYMONT et al., 2013).

Dentro desse cenário os oceanos tropicais têm importância fundamental na regulação do clima, pois atuam como um canal ativo de comunicação entre altas e baixas latitudes (WANG et al., 1999; YU; CHEN, 2013). O Mar Sul da China (SCS) aparece nesse contexto como uma região de grande interesse para as reconstruções paleoceanográficas proporcionando registros marinhos de alta resolução temporal (JIAN, et al., 2000; WANG, et al., 2014). Além disso, esta bacia tropical está sob influência do maior sistema de monção atual (WANG et al., 1999; MCCLYMONT et al., 2013; YU; CHEN, 2013).

Os sistemas de monções são sistemas climáticos de escala global, caracterizados por mudanças sazonais na circulação atmosférica que provocam reversão de ventos e mudanças nos padrões de precipitação continental (HESS; KUHNT, 2005; WANG, 2009; CHENG et al., 2012). Essas alterações ocorrem devido à migração sazonal da Zona de Convergência Intertropical (*Intertropical Convergence Zone* - ITCZ) associada à reversão sazonal da capacidade de aquecimento entre o continente e o oceano (WANG; DING, 2008; CHENG et al., 2012).

O Sistema de Monção Asiático configura o maior sistema de monções atual, com dois subsistemas: o Indiano ou do Sul da Ásia e o do Leste da Ásia. O Sistema de Monção do Leste da Ásia (EAM) influencia significativamente os padrões oceanográficos sazonais do SCS (HESS; KUHNT, 2005; WANG et al., 2005[a,b], 2009; HE; WU, 2013). Durante o inverno, por exemplo, esta bacia marginal do Pacífico Ocidental apresenta variações de até 9º C na temperatura da superfície do mar (*sea surface temperature* - SST) (JIAN et al., 2000, 2001; HESS; KUHNT, 2005).

Apesar das forçantes orbitais apresentarem oscilações semelhantes dentro dos ciclos glaciais-interglaciais do Quaternário, as interações oceano-continente de cada

região e os mecanismos de *feedback* internos podem influenciar de maneira diferente os padrões das monções (WANG, 2009). Assim, a evolução do EAM abrange um amplo espectro de escalas temporais e espaciais, fazendo-se necessária a exploração dessas variações em estudos paleoclimáticos. Assumindo que estas mudanças apresentam padrões recorrentes e naturais, o estudo dos padrões do EAM contribui para o entendimento das mudanças climáticas globais e a predição de cenários futuros, dentro do seu papel de regulação de umidade e calor em baixas latitudes. Além disso, o EAM interfere diretamente no desenvolvimento da produção agrícola da região mais populosa do planeta, que depende da agricultura de subsistência (CHENG et al., 2012; WANG et al., 1999).

Mudanças nas condições hidrográficas das águas superficiais dos oceanos são cruciais para o sistema climático uma vez que afetam interações oceano-atmosfera e o armazenamento de calor (REGENBERG et al., 2009). Desta maneira, a SST aparece como foco de reconstruções paleoceanográficas e paleoclimáticas (WANG; WANG, 1990; WEFER et al., 1999; JIAN et al., 2000). Os foraminíferos planctônicos são amplamente utilizados nessas reconstruções graças a sua ampla distribuição e abundância nos sedimentos marinhos (WEFER et al., 1999; KUCERA et al., 2005; KUCERA, 2007). A sua biodiversidade e distribuição geográfica são controladas pelas interações de parâmetros como temperatura, salinidade e a concentração de nutrientes, de forma que a composição das assembleias de foraminíferos planctônicos permite a interpretação das condições ambientais no momento em que estavam vivos (KUCERA et al., 2005). Com isso, a abundância relativa de foraminíferos planctônicos e a composição de assembleias tem sido aplicada no entendimento dos padrões e evolução da EAM, especialmente no que se refere a sua influência sobre a TSM dentro dos ciclos glaciais-interglaciais do Quaternário (KIENAST, 2001; SHYU et al., 2001; STEINKE et al., 2001; CHEN et al., 2005; ZHENG et al., 2005).

Recentemente, a influência de outras variáveis ambientais (p.e., produção primária (PP)) como fatores de controle na composição de foraminíferos planctônicos, particularmente em oceanos tropicais está em discussão (p.e., MOREY et al., 2005; ZARIC et al., 2005; JONKERS; KUCERA, 2015), e dentro dessa perspectiva o capítulo 1 desta dissertação, "*East Asian Monsoon impacts over the South China Sea mixed layer depth in the last 25ka: A planktonic foraminifera response*" , investigou a influência da dinâmica da profundidade da camada de mistura (*Mixed Layer Depth* – MLD) desde o Último Máximo Glacial (*Last Glacial Maximum* - LGM) sobre os foraminíferos

planctônicos, com base em uma compilação de dados obtidos a partir 11 testemunhos previamente publicados coletados nas sub bacias Norte e Sul do SCS. Neste capítulo, a variabilidade espacial e temporal da MLD em resposta à atividade/intensidade da EAM foi avaliada através das mudanças na porcentagem de foraminíferos planctônicos *deep-dwellers* (habitantes de águas profundas) e de uma Função Empírica Ortogonal (*Empirical Orthogonal Function* - EOF).

No capítulo 2 - "*A 300,000 year record of the East South China Sea sub-basin surface water dynamics: planktonic foraminiferal assemblages"* realizamos a caracterização das assembleias de foraminíferos planctônicos do Hole U1431D, retirado da região de mar profundo da porção central do SCS. As assembleias foram interpretadas de acordo com sua resposta a mudanças na SST e na PP da sub-bacia Leste do SCS. Aos dados de abundância de foraminíferos planctônicos foi aplicada uma função de transferência, com base na Técnica de Análogos Modernos (*Modern Analog Technique* - MAT), para a obtenção de estimativas de SST. A abundância de *deep-dwellers* foi utilizada para reconstrução de variações na MLD.

Os capítulos são apresentados em formato de artigo científico de acordo com as diretrizes estabelecidas pelo Manual do Aluno do Programa de Pós-Graduação em Sistemas Costeiros e Oceânicos - PGSISCO (Art. 5), e pela Resolução do Conselho de Ensino Pesquisa e Extensão - CEPE (65/09, de 30 de outubro de 2009) da Universidade Federal do Paraná. A formatação dos capítulos foi condicionada aos padrões das revistas pretendidas.

REFERÊNCIAS

CHAPORI, N.G.; CHIESSI, C.M.; BICKERT, T.; LAPRIDA, C. Sea-surface temperature reconstruction of the Quaternary Western South Atlantic: New planktonic foraminiferal correlation function. **Palaeogeography, Palaeoclimatology, Palaeoecology**, v. 425, p. 67-75, 2015.

CHENG, H.; SINHA, A.; WANG, X.; CRUZ, F.W.; EDWARDS, R.L. The Global Paleomonsoon as seen through speleothem records from Asian and the Americas. **Climate Dynamics**, v. 39, p. 1045–1062, 2012.

CLEMENS, S.C.; PRELL, W.L.; SUN, Y. Orbital-scale timing and mechanisms driving Late Pleistocene Indo-Asian summer monsoons: Reinterpreting cave speleothem D18O. **Paleoceanography**, v. 25, p. 1–19, 2010.

GUIOT, J.; DE VERNAL, A. Transfer functions: methods for qualitative paleoceanography based on microfossils. In: C. Hillarie-Marcel & A. De Vernal (eds.). **Proxies in Late Cenozoic Paleoceanography**, v. 1, p. 523–563, 2007.

HE, Z.; WU, R. Coupled seasonal variability in the South China Sea. **Journal of Oceanography**, v. 69, p. 57–69, 2013.

HESS, S.; KUHNT, W. Neogene and Quaternary paleoceanographic changes in the southern South China Sea (Site 1143): The benthic foraminiferal record. **Marine Micropaleontology**, v. 54, p. 63–87, 2005.

JIAN, Z.; LI, B.; HUANG, B.; WANG, J. Globorotalia truncatulinoides as indicator of upper-ocean thermal structure during the Quaternary: Evidence from the South China Sea and Okinawa Trough. **Palaeogeography, Palaeoclimatology, Palaeoecology**, v. 162, p. 287–298, 2000.

JIAN, Z.; HUANG, B.; KUHNT, W.; LIN, H-L. Late Quaternary Upwelling Intensity and East Asian Monsoon Forcing in the South China Sea. **Quaternary Research**, v. 55, p. 363–370, 2001.

JONKERS, L.; KUČERA, M. Global analysis of seasonality in the shell flux of extant planktonic Foraminifera. **Biogeosciences**, v. 7, p. 2207-2226, 2015.

KIENAST, M.; STEINKE, S.; STATTEGGER, K.; CALVERT, S.E. Synchronous Tropical South China Sea SST Change and Greenland Warming During Deglaciation. **Science**, v. 291, p. 2132-2134, 2001.

KUCERA, M.; WEINELT, M.; KIEFER, T.; PFLAUMANN, U.; HAYES, A.; WEINELT, M.; CHEN, M-T.; MIX, A.C.; BARROWS, T.T.; CORTIJO, E.; DUPRAT, J.; JUGGINS, S.; WAELBROECK, C. Reconstruction of sea-surface temperatures from assemblages of planktonic foraminifera: Multi-technique approach based on geographically constrained calibration data sets and its application to glacial Atlantic and Pacific Oceans. **Quaternary Science Reviews**, v. 24, SPEC. ISS., p. 951–998, 2005.

KUCERA, M. Chapter Six Planktonic Foraminifera as Tracers of Past Oceanic Environments. v. 1, p. 213–262, 2007.

LANG, N.; WOLFF, E.W. Interglacial and glacial variability from the last 800 ka in marine, ice and terrestrial archives. **Climate of the Past**, v. 7, p. 361–380, 2011.

LI, Q.; WANG, P.; ZHAO, Q.; TIAN, J.; CHENG, X.; JIAN, Z.; ZHONG, G.; CHEN, M. Paleoceanography of the mid-Pleistocene South China Sea. **Quaternary Science Reviews**, v. 27, p. 1217–1233, 2008.

MCCLYMONT, E.L.; SOSDIAN, S.M.; ROSELL-MELÉ, A.; ROSENTHAL, Y. Pleistocene sea-surface temperature evolution: Early cooling, delayed glacial intensification, and implications for the mid-Pleistocene climate transition. **Earth-Science Reviews**, v. 123, p. 173–193, 2013.

MOREY, A.E.; MIX, A.C.; PISIAS, N.G. Planktonic foraminiferal assemblages preserved in surface sediments correspond to multiple environment variables. **Quaternary Science Reviews**, v. 24, p. 925-950, 2005.

SHYU, J-P; CHEN, M-P; SHIEH, Y-T; HUANG, C-K. A Pleistocene paleoceanographic record from the north slope of the Spratly Islands , southern South China Sea. **Marine Micropaleontology**, v. 42, p. 61-93, 2001.

STEINKE, S.; YU, P-S.; KUCERA, M.; CHEN, M-T. No-analog planktonic foraminiferal faunas in the glacial southern South China Sea: Implications for the magnitude of glacial cooling in the western Pacific warm pool. **Marine Micropaleontology**, v. 66, p. 71-90, 2008.

WANG, B.; DING, Q. Global monsoon: dominant mode of annual variation in the tropics. **Dynamics of Atmospheres and Oceans**, v. 44, p. 165–183, 2008.

WANG, L.; SARNTHEIN, M.; ERLENKEUSER, H.; GRIMALT, J.O.; GROOTES, P.; HEILIG, S.; IVANOVA, E.; KIENAST, M.; PELEJERO, C.; PFLAUMANN, U. East Asian monsoon climate during the latePleistocene: High-resolution sediment records from the South China Sea. **Marine Geology**, v. 156, p. 243–282, 1999.

WANG, L.; WANG, P. Late Quaternary paleoceanography of the South China Sea: glacial=interglacial contrasts in an enclosed basin. **Paleoceanography**, v. 5, p. 77–90, 1990.

WANG, P.; CLEMENS, S.; BEAUFORT, L.; BRACONNOT, P.; GANSSEN, G.; JIAN, Z.; KERSHAW, P.; SARNTHEIN, M. Evolution and variability of the Asian monsoon system: state of the art and outstanding issues. **Quaternary Science Reviews**, v. 24, p. 595–629, 2005a.

WANG, P.; LI, Q.; TIAN, J. Pleistocene paleoceanography of the South China Sea: Progress over the past 20 years. **Marine Geology**, v. 352, p. 381–396, 2014.

WANG, Y.; CHENG, H.; EDWARDS, R. L.; HE, Y.; KONG, X.; AN, Z.; WU, J.; KELLY, M. J.; DYKOSKI, C. A.; LI, X. The Holocene Asian monsoon: links to solar

changes and North Atlantic climate. **Science** (New York, N.Y.), v. 308, n. 5723, p. 854–857, 2005b.

WEFER, G.; BERGER, W.H.; BIJMA, J.; FISCHER, G. Clues to Ocean History: a brief overview of proxies. In: Fischer, G.; Wefer, G. (eds.). **Use of Proxies in Paleoceanography - Examples from the South Atlantic**. Berlin Heidelberg: Springer, p. 1-68, 1999.

YU, P.; CHEN, M. Millennial-to-orbital scale changes in the planktic foraminiferal assemblages and sea surface temperature in the South China Sea during the Past 135 Kya. **Geophysical Research Abstracts**, v. 15, p. 9190, 2013.

ZARIC, S., SCHULZ, M., MULITZA, S. Global prediction of planktonic foraminiferal fluxes from hydrographic and productivity data. **Biogeosciences**, v. 55, p. 77-105, 2005.

ZHANG, P. Z.; CHENG, H.; EDWARDS R.L.; CHEN F.H.; WANG Y.J.; YANG X.L.; LIU, J.; TAN, M.; WANG, X.F.; LIU, J.H.; AN, C.L.; DAI, Z.B.; ZHOU, J.; ZHANG, D.Z; JIA, J.H.; JIN, L.Y.; JOHNSON, K.R. A test of climate, sun, and culture relationships from a 1810-year Chinese Cave record. **Science**, v. 322, p. 940-942, 2008.

ZHENG, F.; LI, Q.; LI, B.; CHEN, M.; TU, X.; TIAN, J.; JIAN, Z. A millennial scale planktonic foraminifer record of the mid-Pleistocene climate transition from the northern South China Sea. **Palaeogeography, Palaeoclimatology, Palaeoecology**, v. 223, p. 349-363, 2005.

Capítulo I

East Asian Monsoon impacts over the South China Sea mixed layer depth in the last 25 ka: A planktonic foraminifera response

Amanda Gerotto[a], Renata Hanae Nagai[a]

Potenciais colaboradores: Iván Hernandez-Almeida[b]

[a]Centro de Estudos do Mar, Universidade Federal do Paraná, Av. Beira Mar, s/n, Pontal do Paraná 83255-000, PR Brasil

[b]Marum - Center for Marine Environmental Sciences, University of Bremen, Leobener Str. D-28359, Bremen, Germany

Revista pretendida: Quaternary Science Reviews (Quaternary Sci Rev), ISSN (020773791), Fator de Impacto (JCR, 2015) = 2.928, Qualis CAPES = Biodiversidade A2

Abstract

Here we examine changes in the South China Sea (SCS) upper water column structure over the last 25 ka. For this we compiled a dataset composed of 11 planktonic foraminifera (PF) census records obtained from cores retrieved from the Northern and Southern SCS sub-basins. Mixed layer depth (MLD) changes are reconstructed through the percentage of deep-dwelling PF species in the SCS. We then evaluate MLD spatial-temporal patterns in the SCS through an empirical orthogonal function (EOF) analysis. Our reconstruction points to a deeper MLD during the Last Glacial Maximum (LGM) and Heinrich event 1 (H1), associated to a strengthened East Asian Winter Monsoon (EAWM). Additionally, northern SCS sub-basin MLD presented a more pronounced response to these cool events than its southern counterpart, reflecting the N-S latitudinal influence of the EAWM. During these cold events, the southward shift of the Siberian high-pressure system lead to an intensification of the EAWM winds. This highlights the role of the East Asian Monsoon System in high and low latitude atmospheric connection.

Keywords: Planktonic foraminifera; deep-dwelling species; East Asian Winter Monsoon; Abrupt climatic changes.

1. Introduction

The South China Sea (SCS) is a tropical marginal basin of fundamental importance in the comprehension of the interaction between high and low latitudes climatic processes (Wang et al., 2008; Yu and Chen, 2013). This semi-enclosed basin is characterized by high sedimentation rates, especially during the glacial periods (i.e., 2.5-7.1 cm/ka) (Wang et al., 1995), and good carbonate preservation (Liu et al., 2015). In addition, the SCS is under the influence of a branch of the largest modern monsoon system, the East Asian Monsoon System (EAM), an atmospheric feature with global influence (Zhang et al. 2009; Cheng et al. 2012). Therefore, the sedimentary records of the SCS are an ideal data source for palaeoceanographic and palaeoclimatological reconstructions.

Late Quaternary glacial-interglacial cycles are substantially investigated based on the reconstruction of sea surface temperature (SST) once this variable connects the ocean and the atmosphere, affecting global climate (Kienast 2001; Chen et al. 2005; Oppo and Sun 2005). Planktonic foraminifera (PF) assemblages are widely applied as proxies in these palaeoceanographic reconstructions. Hydrographic conditions (i.e., temperature and salinity), which can be modulated by past climatic oscillations, control these organisms biodiversity and their geographical distribution are controlled (Wefer et al., 1999; Kucera 2007). Although SSTs are the main controlling factor of PF assemblages, other environmental variables are also relevant for assemblage distribution (Schiebel, 2002; Morey et al., 2005; Zaric et al., 2005; Jonkers and Kucera, 2015).

In oligotrophic basins, such as Tropical oceans, for example, the interaction between primary productivity (PP) export flux and seasonal changes of the mixed layer depth (MLD) significantly influence PF test fluxes (Salmon et al., 2015). In Tropical oceans, as a general setting, deeper (shallower) MLD lead to higher (lower) nutrient availability. As a consequence, PP export flux increase (decrease), favoring (hindering) the development of deep-dwelling PF species and test fluxes to the seafloor (Salmon et al., 2015). This relationship allows the application of deep-dwelling PF percentages as a MLD proxy (Andreasen and Ravelo, 1997; Tian et al., 2005).

In the SCS, the MLD responds quickly to ocean-atmosphere interactions as wind stress, and sea-air heat exchange act in the upper-ocean layers creating instability (Duan et al., 2012; Xianjun et al., 2013). EAM winds generate turbulence that affects substantially the exchange of heat and nutrients between the superficial and deeper layers

of the SCS water column through changes in the MLD (Duan et al., 2012; Xianjun et al., 2013). Consequently, the PF fauna will respond to changes in food availability that follow MLD changes. Here we present a MLD reconstruction for the South China Sea spanning the last 25 ka. For this we apply the percentage of deep-dwelling PF from a dataset compiled from previously published SCS records. This dataset comprises 11 records (Figure 1). We also perform an Empirical Orthogonal Function (EOF) in order to understand SCS spatial-temporal MLD patterns. We then use the MLD curve and the EOF results to infer past ocean-atmosphere interactions since the LGM.

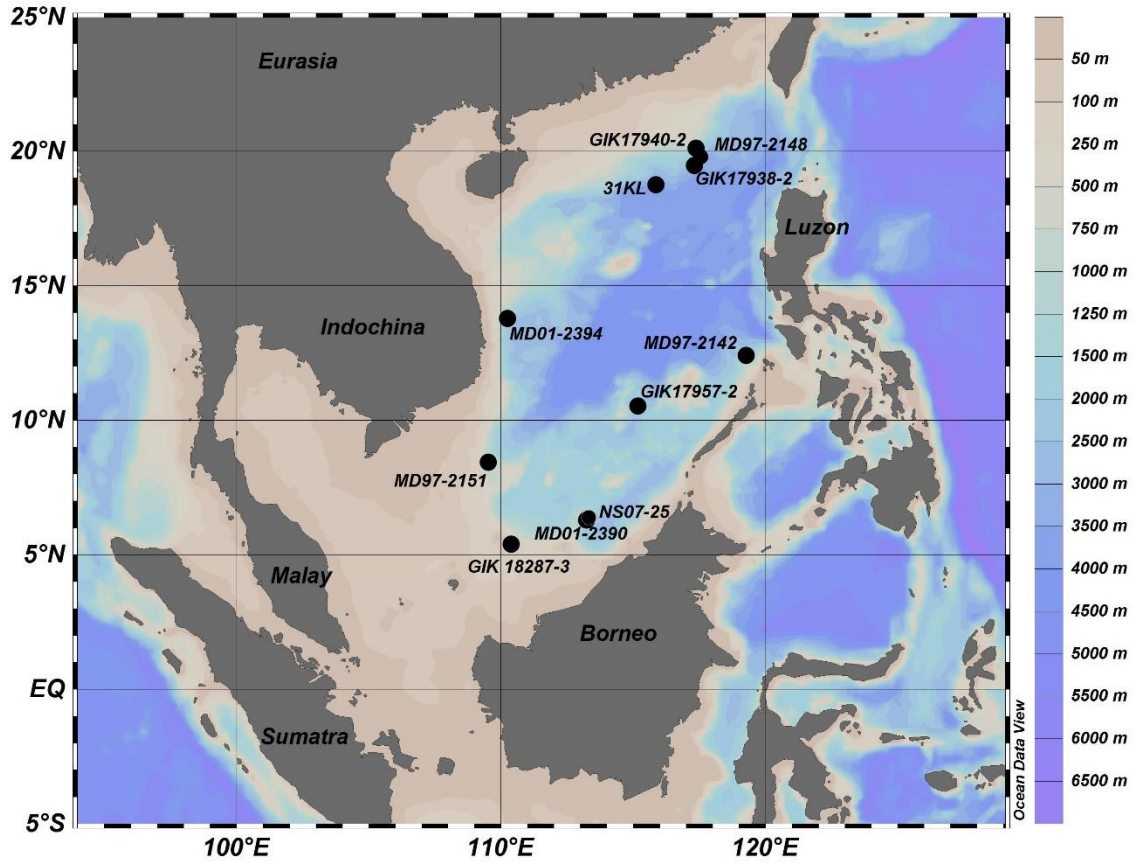

Figure 1. Map of the South China Sea and locations of marine sedimentary records used for the dataset compilation.

2. Regional setting

The South China Sea (SCS), is one of the largest marginal seas in the world, located adjacent to the tropical-to-subtropical western North Pacific (Figure 1). The seasonal reversal of the EAM winds control modern surface water conditions on the NE-SW axis of the SCS (Liu et al., 2004; Liu et al., 2008; Wang and Li, 2009; Li et al., 2014). During the East Asian Winter Monsoon (EAWM), northeasterly winds act from

North to South in the SCS (Wang et al., 1995; Chen et al., 1999; Wang and Li, 2009). Whereas, during the East Asian Summer Monsoon (EASM), relatively weaker southwesterly winds act in the southern and central parts of the SCS (Wang and Li; 2009).

Surface hydrodynamics are characterized by the presence of a large cyclonic gyre during winter, and a weak cyclonic gyre in the North and a strong anticyclonic gyre in the South during summer (Liu et al., 2010). These seasonal variations in the hydrodynamic settings result in contrasting SST and salinity latitudinal patterns (Liu et al., 2008). In summer, the SST is basin wide uniform with small variations (between 28,5-29,5°C); while a large latitudinal SST gradient of approximately 9°C is observed between northern and southern SCS in winter (Liu et al., 2008).

SCS MLD also presents strong spatial-temporal variability, with remarkable seasonal and interannual variations (Duan et al., 2012). MLD climatology is primarily modulated by winds and sea-air heat exchange (Duan et al., 2012). The stronger EAWM winds are able to increase the MLD throughout the SCS (Xianjun et al., 2013). Additionally, the loss of surface heat under lower atmospheric temperature conditions promotes further water column instability making the MLD more susceptible to wind disturbance, under these conditions even weak winds can deepen the MLD (Duan et al., 2012; Xianjun et al., 2013).

3. Material and methods

3.1 Data and chronology

We compiled a dataset based on 11 previously published PF faunal records from the SCS. These records cover a latitudinal and longitudinal range of 5°N to 20°N and 110°W to 119°W, and water depths from 1545 m to 3360 m (Table 1, Figure 1). PF faunal records (>150 µm) were obtained from the Publishing Network for Geoscientific and Environmental Data (PANGAEA – www.pangea.de). Ages obtained from the published records were based on $\delta^{18}O$ stratigraphy or ^{14}C dating (Table 1). To standardize ^{14}C ages were calibrated to calendar years with Calib 7.1 (available at http://calib.qub.ac.uk/calib/). We assumed a reservoir effect of 400yr, corresponding to the Marine13 calibration dataset (Reimer et al., 2013).

Table 1. Site location of the marine sedimentary records comprised in this planktonic foraminifera compilation. Time interval refers to the first and last age of each record, where numbers indicate if age models where based on (1) ^{14}C dating or (2) $\delta^{18}O$ stratigraphy.

Core (ID)	Lat (°N)	Long (°W)	Water depth (m)	Time interval (ka BP)	Number of data points	References
GIK 17940-2	20.11	117.38	1727	0.1 - 24.7[1]	100	Pflaumann and Jian (1999)
MD97-2148	19.79	117.54	2830	0.1 - 24.9[1]	160	Chen et al. (1999)
GIK 17938-2	19.47	117.32	2840	0.3 - 24.9[1]	57	Chen et al. (1999)
31 KL	18.75	115.87	3360	14.4 - 15.9[1]	14	Chen et al. (1998)
MD01-2394	13.78	110.25	2097	0.1 - 24.9[1]	157	Yu et al. (2006)
MD97-2142	12.41	119.27	1557	0.08 - 24.3[2]	39	Chen et al. (2003)
GIK 17957-2	10.53	115.18	2195	0.8 - 22.3[2]	9	Jian et al. (2000)
MD97-2151	8.43	109.51	1589	0.1 - 24.7[1]	82	Huang et al. (2002)
NS07-25	6.39	113.32	2006	2.6 - 24.6[1]	31	Xiang et al. (2009)
MD01-2390	6.28	113.24	1545	1.0 - 24.4[1]	46	Steinke et al. (2008)
GIK 18287-3	5.39	110.39	598	3.3 - 16.6[1]	51	Steinke et al. (2001)

3.2 Deep-dwelling PF as a MLD Index

According to the lifecycles and the depth-related habitat of the PF species, a shallow (deep) MLD will increase the abundance of shallow water (subsurface and deep-dwelling) species (Li, et al., 2004; Tian et al., 2005; Zheng et al., 2005; Steinke et al., 2010; Salmon et al., 2015). This correlation is especially pronounced for deeper-dwelling/subsurface species (Lin and Hsieh, 2007; Salmon et al., 2015), hence the relative abundance of deep-dwelling water species was applied as a MLD proxy. In our composite dataset, deep-dwelling/subsurface species are represented by *Candeina nitida*, *Pulleniatina* spp., *Neogloboquadrina* spp., *Globorotalia* spp (Fairbanks et al., 1982; Li et al., 2004; Kucera, 2007; Schiebel and Hemleben, 2016).

We divided the records into two groups representing the North (records retrieved above 13°N) and South (records retrieved below 13°N) SCS. The records were then stacked to generate two continuous records encompassing the last 25 ka.

3.3 EOF analysis

An unrotated Empirical Orthogonal Function (EOF) analysis was performed to find spatial and temporal patterns within our datasets using the software PAST 3.0 (Paleontology Statistic) (Hammer et al., 2001; Venegas, 2001). The EOF analysis was used to compare the variability of northern and southern cores checking the contribution

of each EOF spatially. This was accomplished by comparing the EOF loadings with others marine and continental records of the EAWM and EASM activity.

The EOF was performed by applying a principal component analysis to a matrix F = M x N where each row represents the measurements for a time tj (j=1,…n) and each column represents a time interval of the investigated sites. To perform the EOF the data set must have the same time spacing (t1 = tn). Hence, records GIK 17940-2, MD97-2148, GIK17938-2, MD01-2394 (representing the northern SCS); and MD9721-42, MD9721-51, NS05-95, MD01-2390 and GIK 18287-3 (representing southern SCS) were interpolated in 100 year intervals using PAST 3.0 (Paleontology Statistic) (Hammer et al., 2001). The 31KL and GIK17857-2 records were excluded for the EOF analysis due to their low temporal resolution.

4. Results and discussion

4.1 Deep-dwelling PF as a MLD Index

The deep-dwelling PF species found in the compiled SCS dataset include *Candeina nitida, Globorotalia crassaformis, Gr. hirsuta, Gr. inflata Gr. menardii, Gr. menardii flexuosa, Gr. scitula, Gr. theyeri, Gr. truncatulinoides, Gr. tumida, Neogloboquadrina dutertrei, N. pachyderma* and *Pulleniatina obliquiloculata*. Based on their depth habitats, these species are classified as intermediate and deep-water dwellers, living below the thermocline (Keller, 1985; Li, 2004; Regenberg et al., 2014). Symbiont-barren and facultative species *C. nitida* and *Neogloboquadrina* spp. inhabit nutrient-enriched waters, with high seafloor test abundances related to regions with enhanced PP (Kuroyanagi and Kawahata, 2004; Jonkers and Kucera, 2015). *Globorotalia* spp. shell flux responds to both SST and PP (Jonkers and Kucera, 2015). While, the facultative symbiont *P. obliquiloculata*, test flux has a positive response to warm subsurface waters (Jonkers and Kučera, 2015; Pflaumann and Jian, 1999). Considering that in the SCS MLD changes affect both food availability and water column temperature (Duan et al., 2012; Xianjun et al, 2013), we assume that changes in the percentage of deep-dwelling PF of our records reflect changes in the MLD.

Our results point to a progressive MLD shoaling in the northern and southern SCS sectors in the last 25 ka (Figure 2). This general trend is superimposed by distinct intervals of deep-dwelling PF percentages change: (i) between 22 and 18 ka corresponding to the Last Glacial Maximum (LGM), (ii) between 17 and 15 ka, Heinrich event 1 (H1), cold

events mainly recorded in the Northern Hemisphere, and (iii) after 15 ka towards the Present (Figure 2).

The LGM is marked by relatively higher deep-dwelling PF percentages, 72.0% and 63.0%, for the northern and southern SCS sectors, respectively (Figure 2), suggesting deeper MLD during the LGM. This scenario is in agreement with PF Mg/Ca based upper-ocean thermal structure reconstructions (Figure 2) (Steinke et al., 2011). During the LGM, streghthened EAWM lead to an overall deeper SCS MLD (Steinke et al., 2011). After the LGM, a progressive MLD shoaling is observed for the northern and southern SCS sectors, but with distinct behaviour during the H1 (Figure 2). After 15 ka a slight decrease in deep-dwelling PF percentages is observed in both northern and southern SCS sectors (Figure 2) suggesting a MLD shoaling towards the Present.

In the northern sector records, both the LGM and the H1 are marked by relatively higher abundance of deep-dwelling PF species (72.0% and 74.0%, respectively). The LGM is followed by an abrupt decrease in deep-dwelling PF species, going from 68.8% to 15.0% from 18 and 17 ka, respectively (Figure 2). Deep-dwelling PF species percentages increase again in the H1, from 7.1% to 41.2%, between 17 and 15 ka, respectively. Meanwhile, in the southern SCS the H1 is marked a sharp decrease in deep-dwelling PF abundances, reaching 7.1% at approximately 15 ka (Figure 2). Hence, during the H1, the the north SCS sub-basin experienced deeper MLD, while in the south SCS sub-basin the H1 was marked by a shallower MLD.

The influence of Northern Hemisphere cold events over the EAM dynamics have been reported in continental records from East Asia suggesting an atmospheric teleconnection between high and low latitudes (Yu et al., 2000; Donghuai, 2004; Guo et al., 2008). Nevertheless, numerical simulations (Yanase and Ouchi, 2007) and proxy based reconstructions (Chen et al., 2003; Sun et al., 2011; Su et al., 2013) point to strong ocean-atmosphere coupling during these climatic events. The EAWM northwesterly winds were intensified by the cold and dryer North Hemisphere (Yanase and Ouchi, 2007; Sun et al., 2011; Wang et al., 2014), and its consequent southward displacement of the Siberian high-pressure system (Chen and Huang, 1998). Thus, our deep-dwelling PF records reflect deeper MLD under intensified EAWM winds under and colder atmospheric temperatures. The abrupt changes recorded in the northern SCS sector and the less pronounced southern SCS may be a consequence of the latitudinal gradient of the EAWM impact, decreasing from N-S basin axis (Qu, 2001; Cheng et al., 2005; Xianjun et al., 2013).

A deeper MLD during the cold events LGM and Younger Dryas was reported by Steinke et al. (2011) in response to strengthened EAWM. However, the differences between northern (MD05-2904) and southern (MD01-2390) SCS sectors is not clear in surface and subsurface temperatures obtained from Mg/Ca ratios from *G. ruber* and *P. obliquiloculata* (Steinke et al., 2011). However, the MLD reconstruction based on deep-dwelling fauna presented signals of both LGM and H1 in the northern sector while the southern sector showed less pronounced changes, except for a contrast of deeper MLD during the LGM followed by a shoaling. As the MLD in the SCS mainly respond to net heat flux and wind surface turbulence our compilation reflect EAWM impacts throughout the N-S SCS axis.

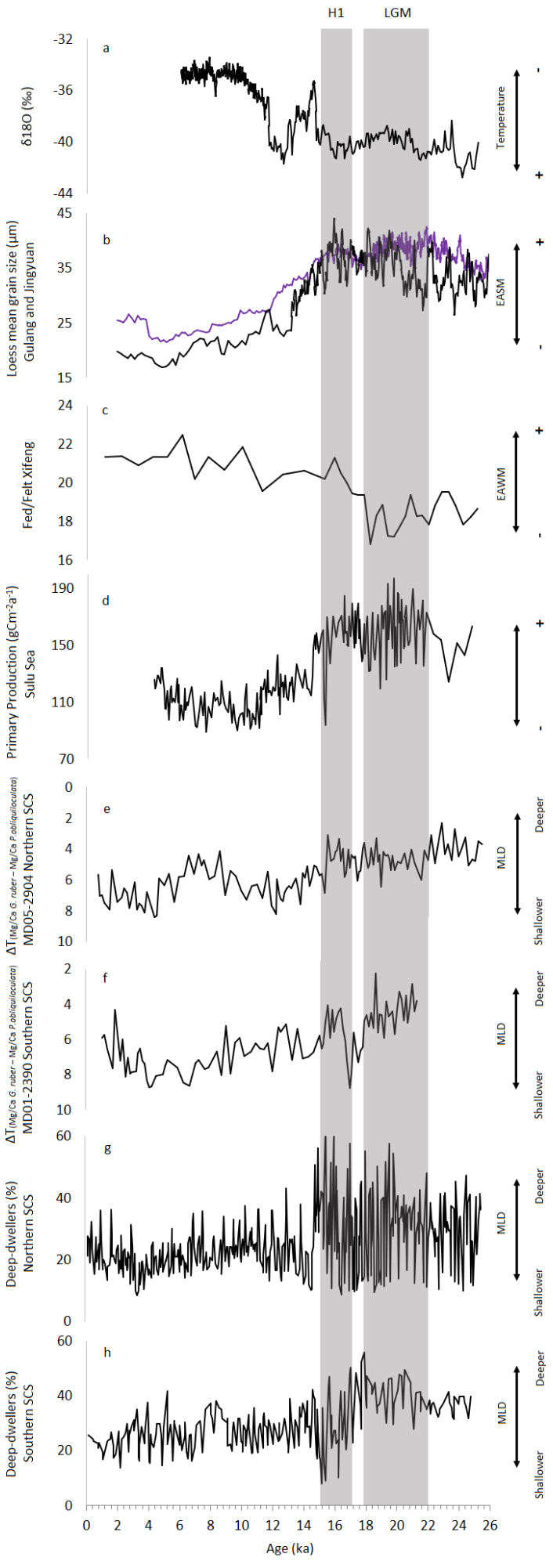

Figure 2. SCS marine records compared with Greenland ice core $\delta^{18}O$ (‰) compared, and EAM continental proxy records. (a) Greenland $\delta^{18}O$ record (Grootes and Stuiver, 1997); (b) Loess mean grain size of Gulang and Jingyuan (Chinese Loess Plateau) (Sun et al., 2011). (c) Fed/Felt from Xifeng loess (chemical weathering) (Guo et al., 2008); (d) Sulu Sea primary productivity (PP, Steinke, and Kienast, 2001) (de Garidel-Thoron et al., 2001); (e) $\Delta T_{(Mg/Ca\ G.\ ruber\ -\ Mg/Ca\ P.obliquiloculata)}$ MD05-2904 (Northern SCS) (Steinke et al., 2011); (f) $\Delta T_{(Mg/Ca\ G.\ ruber\ -\ Mg/Ca\ P.obliquiloculata)}$ MD01-2390 (Southern SCS) (Steinke et al., 2011); (g) Deep-dwelllers (%) variability of northern SCS (this study); (h) Deep-dwelllers (%) variability of southern SCS (this study).

4.2 EOF-analysis

The EOF analysis based on the deep-dwelling PF percentages isolated two principal factors (EOF-1 and EOF-2), that together explain 74.9% of the total variance. EOF-1 mode corresponds to 48.5% of the total variance, and EOF-2, 26.4% (Figure 3). EOF factor loadings variability revealed deep-dwelling PF response to PP (EOF-1) and subsurface water temperatures (EOF-2) (Figure 3). EOF-1 positive (negative) values point high (low) PP, whereas EOF-2 positive (negative) values indicate warm (cold) subsurface temperature. EOF-1 reveals that, in the last 25 ka, deep-dwelling PF from both the northern and southern SCS sectors positively responded to PP enhancement (Figure 4). While, there was no clear response of deep-dwelling PF to subsurface waters temperature, as shown by EOF-2 (Figure 3).

In the modern SCS, PP in both the northern and southern sub-basins is strongly affected by the EAM seasonal dynamics. Our EOF analysis presented two positive EOF-1 intervals (from 25 to 15 ka, and 12 to 10 ka) followed by abrupt decreases in EOF-1 (between 14 and 12 ka, and 10 and 6 ka) (Figure 3). Which suggests an alternation between enhanced and low PP in SCS surface waters within these intervals. This is in agreement with Sulu Sea paleoproductivity records reported by de Garidel-Thoron et al. (2001) (Figure 3). After 6 ka, however, EOF-1 values are persistently negative and with a relatively stable behavior (Figure 3).

EOF-1 highlights enhanced PP particularly during known strengthened EAWM periods, such as the LGM in both northern and southern sectors (de Garidel-Thoron et al., 2001; Steinke et al., 2010). EAWM strong northeasterly winds promote water column mixing and supply surface waters with nutrients consequently, increasing PP (He et al., 2012; Su et al., 2015). While EASM winds promote water column stratification and surface waters nutrient depletion (He et al., 2012; Su et al., 2015). Our records are subjected to coupled effects of both the winter and summer monsoons which may impact SCS productivity differently. Thus, the northern SCS experiences larger PP amplitudes than its southern counterpart (Cheng et al., 2005). Therefore, our EOF-1 response to the Northern Hemisphere cold events is associated with the strength of the EAWM, as corroborated by Sulu Sea PP (Figure 3) (de Garidel-Thoron et al., 2001).

As the EAWM winds promote water column mixing, SCS subsurface temperatures decrease. EOF-2, however, showed no clear spatial pattern, particularly regarding latitudinal differences within SCS N-S axis (Figure 3). EOF-2 negative values

between 25 and 20 ka, and after 10 ka (Figure 3) suggest colder subsurface waters, while positive values observed between 20 and 10 ka point to warmer subsurface waters (Figure 3). Although in agreement with SCS Mg/Ca based subsurface temperature reconstructions (Steinke et al., 2011), these intervals do not coincide with known climatic events, such as the LGM or H1 (Figure 3). Assuming that EOF-2 represents deep-dwelling PF response to subsurface temperatures, this implies that SCS subsurface temperatures are driven by a different mechanism than the EAM. These mechanisms could be related to one of the multiple physical processes that influence SCSs' upper-ocean structure, such as (i) upwelling activity or (ii) changes in the circulation from exchange waters of Western Pacific, through the Kuroshio Current (He et al., 2013).

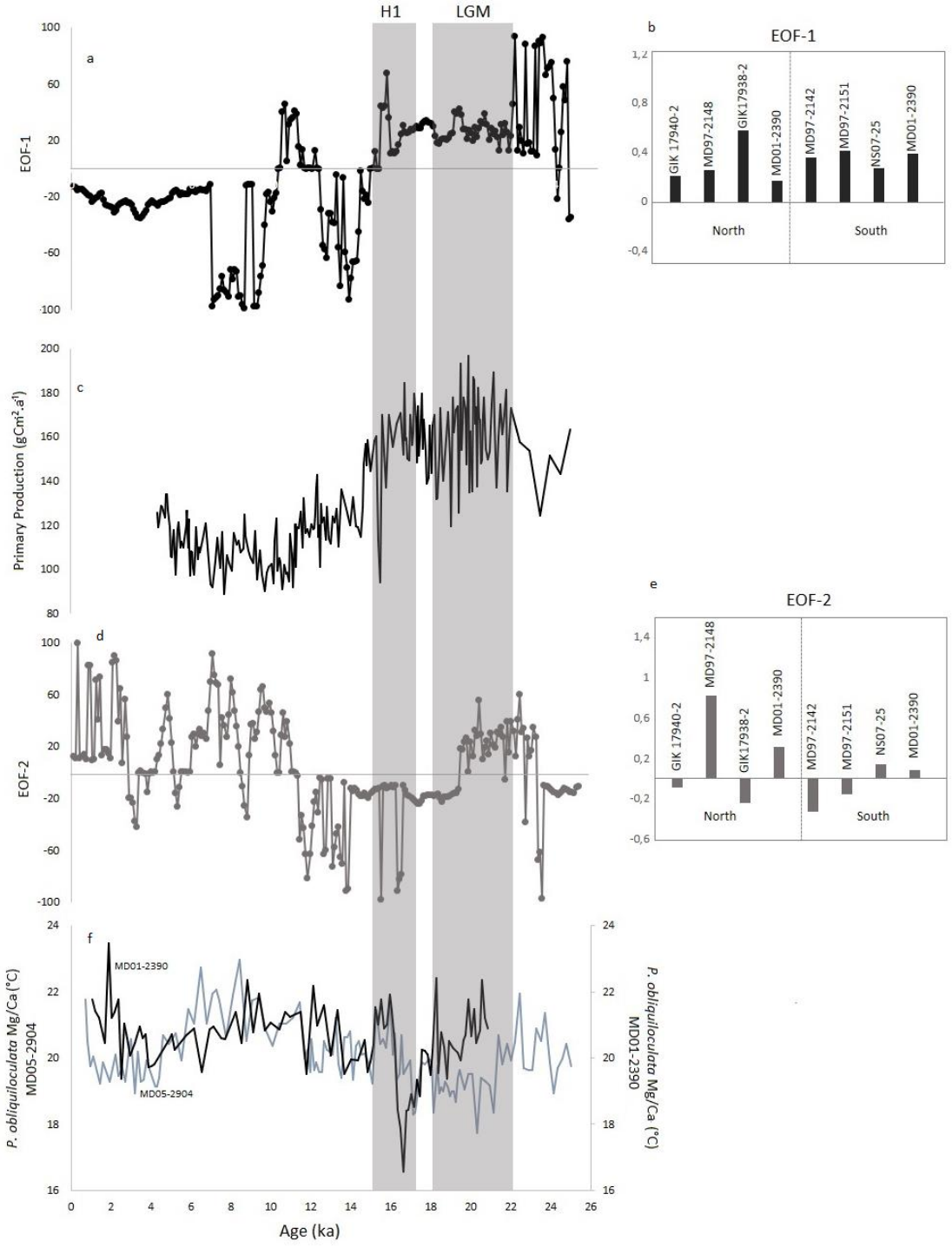

Figure 3. EOF variability of the southern and northern SCS sectors responding to primary productivity and subsurface temperatures. (a) EOF-1 loadings over the last 25 ka (this study); (b) EOF components correspondent to deep-dwelling abundance (%) in the northern SCS; (c) Sulu Sea primary productivity (de Garidel-Thoron et al., 2001); (d) EOF-2 loadings over the last 25 ka records (this study); (e) EOF components correspondent to deep-dwelling abundance (%) in the southern SCS; and (f) Subsurface temperatures based on Mg/Ca rations from *P. obliquiloculata* from MD05-2904 (northern SCS) and MD01-2390 (southern SCS) (Steinke et al., 2011).

5. Conclusions

The link between the EAM variability and cold events in the North Hemisphere have been previously explored in East Asia continental records. Our new SCS deep-dwelling PF record provides an additional marine proxy based reconstruction to better comprehend interhemispheric atmospheric teleconnections between high and low latitudes during the LGM and H1, particularly observed in the Northern Hemisphere. Additionally, it provides new insights on the impacts of the ocean-atmospheric coupling between the SCS and the strength of the EAWM winds.

Acknowledgements

The authors would like to thank Coordenação de Aperfeiçoamento de Nível Superior (CAPES) for the MSc scholarship granted to Amanda Gerotto and to the Graduate Program in Ocean and Coastal Systems (PGSISCO) of Federal University of Paraná (UFPR). We are also in debt with Dr. Min-T Chen and Dr. Pai-Sen Yu for providing MD9721-48, and MD01-2394 datasets.

References

Andreasen, D.J. and Ravelo, A.C. (1997). Tropical Pacific Ocean thermocline reconstructions for the last glacial maximum. *Paleoceanography, 12*(3), 395–413. http://dx.doi.org/10.1029/97PA00822

Chen, M.T., Huang, C.C., Pflaumann, U., Waelbroeck, C. and Kucera, M. (2005). Estimating glacial western Pacific sea-surface temperature: methodological overview and data compilation of surface sediment planktic foraminifer faunas. *Quaternary Science Reviews*, *24*(7–9), 1049–1062. http://doi.org/http://dx.doi.org/10.1016/j.quascirev.2004.07.013

Chen, M.T., Wang, P., Wang, L., Sarnthein, M., Wang, C.H. and Huang, C.Y. (1999). A late Quaternary planktonic foraminifer faunal record of rapid climatic changes from the South China Sea. *Marine Geology*, *156*(1-4), 85–108. http://doi.org/10.1016/S0025-3227(98)00174-1

Chen, M.T. and Huang, C.Y. (1998). Ice-volume forcing of winter monsoon climate in the South China Sea. *Paleoceanography*, *13*(6), 622–633. http://doi.org/10.1029/98PA02356

Chen, M.T., Shiau, L.-J., Yu, P.S., Chiu, T.C., Chen, Y.G. and Wei, K.Y. (2003). 500 000-Year records of carbonate, organic carbon, and foraminiferal sea-surface temperature from the southeastern South China Sea (near Palawan Island). *Palaeogeography, Palaeoclimatology, Palaeoecology*, *197*(1-2), 113–131. http://doi.org/10.1016/S0031-0182(03)00389-4

Cheng, H., Sinha, A., Wang, X., Cruz, F. and Edwards, R.L. (2012). The Global Paleomonsoon as seen through speleothem records from Asia and the Americas. *Climate Dynamics*, 39 (5), 1045–1062. http://doi.org/10.1007/s00382-012-1363-7

Cheng, X., Huang, B., Jian, Z., Zhao, Q., Tian, J. and Li, J. (2005). Foraminiferal isotopic evidence for monsoonal activity in the South China Sea: A present-LGM comparison. *Marine Micropaleontology*, *54*(1-2), 125–139. http://doi.org/10.1016/j.marmicro.2004.09.007

de Garidel-Thoron, T., Beaufort, L., Linsley, B. K. and Dannenmann, S. (2001). Millennial-scale dynamics of the East Asian winter monsoon during the last 200,000 years. *Paleoceanography*, *16*(5), 491–502. http://doi.org/10.1029/2000PA000557

Donghuai, S. (2004). Monsoon and westerly circulation changes recorded in the late Cenozoic aeolian sequences of Northern China. *Global and Planetary Change*, 41, 63–80. http://doi.org/10.1016/j.gloplacha.2003.11.001

Duan, R., Yang, K., Ma, Y. and Hu, T. (2012). A study of the mixed layer of the South China Sea based on the multiple linear regression. *Acta Oceanologica Sinica*, *31*(6), 19–31. http://doi.org/10.1007/s13131-012-0250-8

Fairbanks, R. G., Sverdlove, M., Free, R., Wiebe, P. H. and Bé, A.W.H. (1982). Vertical distribution and isotopic fractionation of living planktonic foraminifera from the Panama Basin. *Nature, 298*, 841–844. http://doi.org/10.1038/298841a0

Grootes, P. M. and Stuiver, M. (1997). Oxygen 18/16 variability in Greenland snow and ice with 10 -3- to 105-year time resolution. *Journal Of Geophysical Research*, *102*(C12), 455-470. http://doi.org/10.1029/97JC00880

Guo, Z.T., Berger, a., Yin, Q.Z. and Qin, L. (2008). Strong asymmetry of hemispheric climates during MIS-13 inferred from correlating China loess and Antarctica ice records. *Climate of the Past Discussions*, *5*(21-31), 1061–1088. http://doi.org/10.5194/cpd-4-1061-2008

Hammer, O., Harper, D.A.T. and Rian, P.D. (2001). Past. Palaeonthological statistics software package for education and data analysis. Version. 2.17.

He, J., Zhao, M., Wang, P., Li, L. and Li, Q. (2013). Changes in phytoplankton productivity and community structure in the northern South China Sea during the past 260 ka. *Palaeogeography, Palaeoclimatology, Palaeoecology*, *392*, 312–323. http://doi.org/10.1016/j.palaeo.2013.09.010

He, Z. and Wu, R. (2013). Coupled seasonal variability in the South China Sea. *Journal of Oceanography*, *69*(1), 57–69. http://doi.org/10.1007/s10872-012-0157-1

Hess, S. and Kuhnt, W. (2005). Neogene and Quaternary paleoceanographic changes in the southern South China Sea (Site 1143): The benthic foraminiferal record. *Marine Micropaleontology*, 54(1-2), 63–87. http://doi.org/10.1016/j.marmicro.2004.09.004

Jian, Z., Huang, B., Kuhnt, W. and Lin, H.-L. (2001). Late Quaternary Upwelling Intensity and East Asian Monsoon Forcing in the South China Sea. *Quaternary Research*, *55*(3), 363–370. http://doi.org/DOI: 10.1006/qres.2001.2231

Jian, Z., Li, B., Huang, B. and Wang, J. (2000). Globorotalia truncatulinoides as indicator of upper-ocean thermal structure during the Quaternary: Evidence from the South China Sea and Okinawa Trough. *Palaeogeography, Palaeoclimatology, Palaeoecology*, *162*(3-4), 287–298. http://doi.org/10.1016/S0031-0182(00)00132-2

Jonkers, L. and Kučera, M. (2015). Global analysis of seasonality in the shell flux of extant planktonic Foraminifera. *Biogeosciences*, *12*(7), 2207–2226. http://doi.org/10.5194/bg-12-2207-2015

Keller, G. (1985). Depth stratification of planktonic foraminifers in the Miocene ocean. In Kennett, J.P. (Ed.), The Miocene Ocean: Paleoceanography and Biogeography. *Geologycal Society of America*, *163*, 177-196. http://doi.org/10.1130/MEM163-p177

Kienast, M. (2001). Synchronous Tropical South China Sea SST Change and Greenland Warming During Deglaciation. *Science*, *291*(5511), 2132–2134.

http://doi.org/10.1126/science.1057131

Kucera, M. (2007). Chapter Six Planktonic Foraminifera as Tracers of Past Oceanic Environments, *1*(07), 213–262. http://doi.org/10.1016/S1572-5480(07)01011-1

Kucera, M., Weinelt, M., Kiefer, T., Pflaumann, U., Hayes, A., Weinelt, M., … Waelbroeck, C. (2005). Reconstruction of sea-surface temperatures from assemblages of planktonic foraminifera: Multi-technique approach based on geographically constrained calibration data sets and its application to glacial Atlantic and Pacific Oceans. *Quaternary Science Reviews*, *24*(7-9 SPEC. ISS.), 951–998. http://doi.org/10.1016/j.quascirev.2004.07.014

Kuroyanagi, A. and Kawahata, H. (2004). Vertical distribution of living planktonic foraminifera in the seas around Japan. *Marine Micropaleontology*, *53*(1-2), 173–196. http://doi.org/10.1016/j.marmicro.2004.06.001

Lang, N. and Wolff, E. W. (2011). Interglacial and glacial variability from the last 800 ka in marine, ice and terrestrial archives. *Climate of the Past*, *7*(2), 361–380. http://doi.org/10.5194/cp-7-361-2011

Li, B., Wang, J., Huang, B., Li, Q., Jian, Z., Zhao, Q., Su, X. and Wang P. (2004). Correction to "South China Sea surface water evolution over the last 12 Myr: A south-north comparison from Ocean Drilling Program Sites 1143 and 1146." *Paleoceanography*, *19*(1), 1–12. http://doi.org/10.1029/2004PA001016

Li, C.-F., Xu, X., Lin, J., Sun, Z., Zhu, J., Yao, Y., … Zhang, G.-L. (2014). Ages and magnetic structures of the South China Sea constrained by deep tow magnetic surveys and IODP Expedition 349. *Geochemistry, Geophysics, Geosystems*, *15*(12), 4958–4983. http://doi.org/10.1002/2014GC005567

Lin, H.-L. and Hsieh, H.-Y. (2007). Seasonal variations of modern planktonic foraminifera in the South China Sea. *Deep Sea Research Part II: Topical Studies in Oceanography*, 54(14-15), 1634–1644. http://doi.org/10.1016/j.dsr2.2007.05.007

Liu, Q., Jiang, X., Xie, S. P. and Liu, W. T. (2004). A gap in the Indo-Pacific warm pool over the South China Sea in boreal winter: Seasonal development and interannual variability. *Journal of Geophysical Research C: Oceans*, *109*(#16), 1–10. http://doi.org/10.1029/2003JC002179

Liu, Q., Kaneko, A. and Su, J. (2008). Recent progress in studies of the South China Sea circulation. *Journal of Oceanography*, *64*(5), 753–762. http://doi.org/10.1007/s10872-008-0063-8

Liu, Z., Colin, C., Li, X., Zhao, Y., Tuo, S., Chen, Z., … Huang, K.-F. (2010). Clay mineral distribution in surface sediments of the northeastern South China Sea and surrounding fluvial drainage basins: Source and transport. *Marine Geology*, *277*(1-4), 48–60. http://doi.org/10.1016/j.margeo.2010.08.010

Liu, Z., Zhao, Y., Colin, C., Stattegger, K., Wiesner, M. G., Huh, C.-A., … Li, Y. (2015). Source-to-Sink transport processes of fluvial sediments in the South China Sea. *Earth-Science Reviews*, *153*, 238-273. http://doi.org/10.1016/j.earscirev.2015.08.005

McClymont, E.L., Sosdian, S.M., Rosell-Melé, A. and Rosenthal, Y. (2013). Pleistocene sea-surface temperature evolution: Early cooling, delayed glacial intensification, and implications for the mid-Pleistocene climate transition. *Earth-Science Reviews*, *123*, 173–193. http://doi.org/10.1016/j.earscirev.2013.04.006

Morey, A. E., Mix, A. C. and Pisias, N. G. (2005). Planktonic foraminiferal assemblages preserved in surface sediments correspond to multiple environment variables. *Quaternary Science Reviews*, 24(7-9 SPEC. ISS.), 925–950. http://doi.org/10.1016/j.quascirev.2003.09.011

Oppo, D.W. and Sun, Y. (2005). Amplitude and timing of sea-surface temperature change

in the northern South China Sea : Dynamic link to the East Asian monsoon. *Geological Society of America*, *33*(10), 785-788. http://doi.org/10.1130/G21867.1

Pflaumann, U. and Jian, Z. (1999). Modern distribution patterns of planktonic foraminifera in the South China Sea and western Pacific : a new transfer technique to estimate regional sea-surface temperatures. *Marine Geology*, *156*(1-4), 41–83. http://doi.org/10.1016/S0025-3227(98)00173-X

Qu, T. (2001). Role of ocean dynamics in determining the mean seasonal cycle of the South China Sea surface temperature, *106*(C4), 6943–6955. http:// doi/10.1029/2000JC000479

Regenberg, M., Regenberg, A., Garbe-Schönberg, D. and Lea, D.W. (2014). Global dissolution effects on planktonic foraminiferal Mg/Ca ratios controlled by the calcite-saturation state of bottom waters. *Paleoceanography*, *29*(3), 127–142. http://doi.org/10.1002/2013PA002492

Reimer, P.J., Bard, E., Bayliss, A., Beck, J.W., Blackwell, P.G. and Ramsey, C.B. (2013). IntCal13 and Marine13 Radiocarbon Age Calibration Curves 0–50,000 Years cal BP. *Radiocarbon*, *55*(4), 1869–1887. http://doi.org/10.2458/azu_js_rc.55.16947

Salmon, K. H., Anand, P., Sexton, P.F. and Conte, M. (2015). Upper ocean mixing controls the seasonality of planktonic foraminifer fluxes and associated strength of the carbonate pump in the oligotrophic North Atlantic. *Biogeosciences*, *12*(1), 223–235. http://doi.org/10.5194/bg-12-223-2015

Schiebel, R. 2002. Planktic foraminiferal sedimentation and the marine calcite budget. *Global Biogeochemical Cycles*, *16*(4), 3-1-3-21. http://doi.org/10.1029/2001GB001459

Schiebel, R. and Hemleben, C. (2016). Planktic Foraminifers in the Modern Ocean: Ecology, Biogeochemistry, and Application. Springer. ISBN 3662502976, 9783662502976, 333 p.

Siswanto, E., Ye, H., Yamazaki, D. and Tang, D.L. (2017), Detailed spatiotemporal impacts of El Niño on phytoplankton biomass in the South China Sea. *Journal of Geophysical Research: Oceans*, *122*(4), 1-15. http://doi.org/10.1002/2016JC012276

Steinke, S., Kienast, M., Pflaumann, U. and Weinelt, M. (2001). A High-Resolution Sea-Surface Temperature Record from the Tropical. *Quaternary Research*, *55*(3), 352–362. http://doi.org/10.1006/qres.2001.2235

Steinke, S., Mohtadi, M., Groeneveld, J., Lin, L.C., Löwemark, L., Chen, M.T. and Bühring, R.R. (2010). Reconstructing the southern South China Sea upper water column structure since the Last Glacial Maximum : Implications for the East Asian winter monsoon development. *Paleoceanograohy*, *25*(2), 1–15. http://doi.org/10.1029/2009PA001850

Steinke, S., Glatz, C., Mohtadi, M., Groeneveld, J., Li, Q. and Jian, Z. (2011). P ast dynamics of the East Asian monsoon: No inverse behaviour between the summer and winter monsoon during the Holocene. *Global and Planetary Change*, *78*(3-4), 170-177. http://doi.org/10.1016/j.gloplacha.2011.06.006

Su, X., Liu, C., Beaufort, L., Barbarin, N. and Jian, Z. (2015). Differences in Late Quaternary primary productivity between the western tropical Pacific and the South China Sea: Evidence from coccoliths. *Deep-Sea Research Part II: Topical Studies in Oceanography*, *122*, 131–141. http://doi.org/10.1016/j.dsr2.2015.07.008

Su, X., Liu, C., Beaufort, L., Tian, J. and Huang, E. (2013). Late Quaternary coccolith records in the South China Sea and East Asian monsoon dynamics. *Global and Planetary Change*, *111*, 88–96. http://doi.org/10.1016/j.gloplacha.2013.08.016

Sun, Y., Clemens, S.C., Morrill, C., Lin, X., Wang, X. and An, Z. (2011). Influence of Atlantic meridional overturning circulation on the East Asian winter monsoon.

Nature Geoscience, *5*(1), 46–49. http://doi.org/10.1038/ngeo1326

Tian, J., Wang, P.X., Chen, R.H. and Cheng, X.R. (2005). Quaternary upper ocean thermal gradient variations in the South China Sea: Implications for east Asian monsoon climate. *Paleoceanography*, *20*(4), 1-8. http://doi.org/10.1029/2004PA001115

Venegas, S. A. (2001). Statistical Methods for Signal Detection in Climate. University of Copenhagen, Copenhagen, Denmark, 96 pp.

Wang, L., Sarnthein, M., Erlenkeuser, H., Grimalt, J.O., Grootes, P., Heilig, S., … Pflaumann, U. (1999). East Asian monsoon climate during the latePleistocene: High-resolution sediment records from the South China Sea. *Marine Geology*, *156*(1-4), 243–282. http://dx.doi.org/10.1016/S0025-3227(98)00182-0

Wang, P., Clemens, S., Beaufort, L., Braconnot, P., Ganssen, G., Jian, Z., … Sarnthein, M. (2005). Evolution and variability of the Asian monsoon system: state of the art and outstanding issues. *Quaternary Science Reviews*, *24*(5-6), 595–629. http://doi.org/10.1016/j.quascirev.2004.10.002

Wang, P., Li, Q. and Tian, J. (2014). Pleistocene paleoceanography of the South China Sea: Progress over the past 20 years. *Marine Geology*, 352, 381–396. http://doi.org/10.1016/j.margeo.2014.03.003

Wang, P., Wang, L., Bian, Y. and Jian, Z. (1995). Late Quaternary paleoceanography of the South China Sea: surface circulation and carbonate cycles. *Marine Geology*, *127*(1–4), 145–165. http://doi.org/10.1016/0025-3227(95)00008-M

Wang, Y., Cheng, H., Edwards, R.L., Kong, X., Shao, X., Chen, S., … An, Z. (2008). Millennial- and orbital-scale changes in the East Asian monsoon over the past 224,000 years. *Nature*, *451*(7182), 1090–1093. http://doi.org/10.1038/nature06692

Wefer G., Berger W.H., Bijma J. and Fisher G. (1999). Clues to ocean history: A brief overview of proxies. In: Fisher, G. and Wefer, G. eds.. Use of proxies in paleoceanography: Examples from South Atlantic. Springer-Verlag, Berlin, Heidelberg. http://doi.org/10.1007/978-3-642-58646-0_1

Xianjun, X., Dongxiao, W., Wen, Z., Zuqiang, Z., Yinghao, Q.I.N., Na, H.E. and Lili, Z. (2013). Impacts of a wind stress and a buoyancy flux on the seasonal variation of mixing layer depth in the South China Sea. *Acta Oceanologica Sinica*, *32*(9), 30–37. http://doi.org/10.1007/s13131-013-0349-6

Yanase, W. and Ouchi, A. (2007). The LGM surface climate and atmospheric circulation over East Asia and the North Pacific in the PMIP2 coupled model simulations. *Climate of the Past, 3,* 439–451. http://doi.org/10.5194/cp-3-439-2007

Yu, G., Chen, X., Ni, J., Cheddadi, R., Guiot, J., Han, H., … Huang, C. (2000). Palaeovegetation of China : a pollen data-based synthesis for the mid-Holocene and last glacial maximum. *Journal of Biogeography*, *27*(3), 635–664. http://doi.org/10.1046/j.1365-2699.2000.00431.x

Yu, P.-S. and Chen, M. (2013). Millennial-to-orbital scale changes in the planktic foraminiferal assemblages and sea surface temperature in the South China Sea during the past 135 kya. *Geophysical Research Abstracts, 15,* 9190.

Yu, P.-S., Huang, C.-C., Chin, Y., Mii, H.-S. and Chen, M.-T. (2006). Late Quaternary East Asian Monsoon variability in the South China Sea: evidence from planktonic foraminifera faunal and hydro- graphic gradient records. *Palaeogeography, Palaeoclimatology, Palaeoecology*, *236*(1-4), 74-90. http://doi.org/10.1016/j.palaeo.2005.11.038

Zaric, S., Donner, B., Fischer, G., Mulitza, S. and Wefer, G. (2005). Sensitivity of planktic foraminifera to sea surface temperature and export production as derived from sediment trap data. *Marine Micropaleontology 55*(1-2), 75–105.

http://doi.org/10.1016/j.marmicro.2005.01.002

Zhang, L., Chen, M., Xiang, R., Zhang, L. and Lu, J. (2009). Marine Micropaleontology Productivity and continental denudation history from the South China Sea since the late Miocene. *Marine Micropaleontology*, *72*(1-2), 76–85. http://doi.org/10.1016/j.marmicro.2009.03.006

Zheng, F., Li, Q., Li, B., Chen, M., Tu, X., Tian, J. and Jian, Z. (2005). A millennial scale planktonic foraminifer record of the mid-Pleistocene climate transition from the northern South China Sea. *Palaeogeography, Palaeoclimatology, Palaeoecology*, *223*(3–4), 349–363. http://doi.org/http://dx.doi.org/10.1016/j.palaeo.2005.04.018

Capítulo II

A 300,000 year record of the East South China Sea sub-basin surface water dynamics: planktonic foraminiferal assemblages

Amanda Gerotto[a], Renata Hanae Nagai[a]

Potenciais colaboradores: Rubens C. L. Figueira[b], Paulo A. L. Ferreira[b], Iván Hernandez-Almeida[c]

[a]Centro de Estudos do Mar, Universidade Federal do Paraná, Av. Beira Mar, s/n, Pontal do Paraná 83255-000, PR Brasil

[b]Instituto Oceanográfico, Universidade de São Paulo, Praça do Oceanográfico, 191, São Paulo, Brasil

[c]Center for Marine Environmental Sciences, University of Bremen, Leobener Str. D-28359, Bremen, Germany

Revista pretendida: Marine Micropaleontology (MarMicropaleontol), ISSN (0377-8398), Fator de Impacto (JCR, 2016) = 1.859, Qualis CAPES = Biodiversidade B1

Abstract

This work seeks to better understand the mechanisms that influenced the East South China Sea (SCS) sub-basin surface waters conditions over the last 300 ka. To achieve this, we examined planktonic foraminifera (PF) assemblages regarding their response to sea surface temperature (SST) and primary productivity (PP) changes. A Modern Analogue Technique was applied to the PF fauna data to reconstruct SST, and the percentage of deep-dwelling PF species was used as a proxy of PP. During interglacial stages the East SCS sub-basin surface waters were dominated by *P. obliquiloculata, Gr. menardii, Gs. ruber* (white), *Gs. sacculifera, N. dutertrei, G. rubescens*. These species presence suggests warm and oligotrophic surface waters, and a well-stratified water column, under strengthened East Asian Summer Monsoon (EASM). Interglacial stages high sea-level conditions also favored the exchange of waters between the western Pacific and the SCS, through the Kuroshio Current (KC) inflow into the SCS. The supply of nutrients by the KC inflow enhanced PP at specific interglacial intervals marked by the presence of *G. falconensis, Ga. calida, N. pachyderma, N. incompta* and *Ga. bulloides*. Meanwhile,

glacial stages were characterized by the presence of cold and nutrient-enriched surface waters, with a relatively less stratified water column, related to the strength of the East Asian Winter Monsoon (EAWM). Our data highlights strong regional differences between the SCS sub-basins driven by the East Asian Monsoon and the communication of this marginal basin with the Pacific Ocean.

Keywords: Kuroshio Current; East Asian Monsoon; Sea level; Surface temperature; Productivity.

1. Introduction

The South China Sea (SCS) has a great potential to provide geological data that can be applied in the comprehension of the late Quaternary climatic changes. This marginal sea has high sedimentation rates and a major role in the heat exchange processes between low and high latitudes (Wang et al., 1999; Yu and Chen, 2013). Similarly, in the atmosphere, the East Asian Monsoon System (EAM) is one of the primary mechanisms that enables this communication (Wang et al., 1999; McClymont et al., 2013; Yu and Chen, 2013). The seasonal wind reversal derived from the EAM substantially affect SCS surface waters hydrographic conditions, mainly through changes in air-sea net heat flux (Liu et al., 2008; Wang and Li, 2009; Xianjun et al., 2013).

This marginal basin sea surface temperature (SST) changes have been the focus of planktonic foraminifera (PF) based reconstructions for Quaternary glacial and interglacial cycles (i.e., Steinke, 2001; Chen, 2005; Li et al., 2008; Yu, 2008). PF assemblages or isotopic composition are widely used in palaeoceanographic reconstructions once their abundance and biodiversity are controlled by surface hydrography conditions (Wefer et al., 1999; Kucera, 2007; Dong et al., 2015). PF community structure and geographical distribution, however, are also controlled by other environmental parameters such as primary productivity (PP), salinity and water column thermal structure (Schiebel et al., 2002; Morey et al., 2005; Zaric et al., 2005; Jonkers and Kucera, 2015; Salmon et al., 2015). The seasonality of the PF shell flux has been reported strongly related to the PP cycles, according to ecological preferences of the species (Kucera, 2007; Jonkers and Kucera, 2015; Salmon et al., 2015).

In subtropical oligotrophic seas, such as the SCS, PP is driven by nutrient availability in the euphotic zone. In the SCS multiple mechanisms (e.g., EAM dynamics, upwelling activity, aeolian or river input) can promote nutrient enrichment in surface

waters (Chen et al., 2006; Yu et al., 2008; He et al., 2013; Su et al., 2013). Previous SCS reconstructions report enhanced (reduced) PP during glacial (interglacial) stages as a response to the strong (weak) vertical mixing of the water column leading to a deeper (shallower) mixed layer depth (MLD) promoted by the strengthened East Asian Winter Monsoon (EAWM) (East Asian Summer Monsoon (EASM)) (Tian et al., 2005; He et al., 2013; Su et al., 2013; Su et al., 2015).

The SCS palaeoceanographic records have been widely used for late Quaternary reconstructions since ODP Leg 184 in the late 90s, with the northern and southern SCS sub-basins SST changes in response to the EAM as the main focus of these reconstructions. For the eastern SCS sub-basin, however, only a few studies have been conducted (Chen et al., 2003; Wei et al., 2003; Ren et al., 2012; Li et al., 2017) all based on one record (core MD97-2142). Here we present a new PF record from a record (Hole U1431D) retrieved from the East SCS sub-basin deep-sea during International Ocean Discovery Program (IODP) Expedition 349. Changes in PF assemblages were examined regarding their relationship with SST and PP changes in response to palaeoceanographic and palaeoclimatological oscillations in the last 300 ka.

2. Modern oceanographic conditions

The modern SCS presents significant meridional and zonal hydrographic gradients that determine unique characteristics to this marginal sea sub-basins (Cheng et al., 2005; Xianjun et al., 2013). The oceanographic patterns of the SCS (*i.e.*, SST, surface currents and water column stratification) respond to the seasonal EAM dynamics and the exchange of water with the Pacific Ocean through the Kuroshio Current (KC) (Wang et al., 2009; Liu et al., 2010; He and Wu, 2013).

The EAM seasonal wind reversal is a consequence of the seasonal migration of the Intertropical Convergence Zone and the reversal of the heating capacity between land and ocean (Wang and Ding, 2008; Cheng et al., 2012). During the EASM the SCS surface waters present uniformly high SST (28-29°C) and low salinities due to increased precipitation over the Asian continent (Steinke et al., 2006; Wang and Li, 2009). SW winds, established during May-September mainly in the south and central parts of SCS, reach up to 6 $m.s^{-1}$ (Steinke et al., 2006; Liu et al., 2008; Wang and Li, 2009). Whereas, during the EAWM cold and dry air masses from Siberia, configure low SST (6-21°C) and a large cyclonic gyre in central SCS, as strong winds (>8 $m.s^{-1}$) act in the NE-SW axis of this marginal basin (Steinke et al., 2006; Liu et al., 2008; Wang and Li, 2009). The

latitudinal impact of the EAWM affects the zonal SST gradient, presenting lower temperatures in the northern (20 – 28°C) in contrast to southern SCS (26 – 29,8°C) (Tian et al., 2010).

The variations of the MLD in the SCS reflect the latitudinal and longitudinal gradients of the EAM and SST (Qu, 2001; Xianjun et al., 2013). In the modern SCS, the MLD varies between 15 m and 40 m in the N-S axis during summer (warmer SST) and winter (colder SST), respectively (Chen et al., 1999; Xianjun et al., 2013). The dynamics of the SCS MLD is mainly controlled by air-sea interactions (Duan et al., 2012). However, the northern, southern and western SCS sub-basins MLD changes are profoundly impacted by the EAM wind stress (Xianjun et al., 2003; Cheng et al., 2005). While in the east the overlying atmosphere temperatures, and resulting heat flux, exerts the primary control over MLD and the EAM wind stress plays a secondary role (Xianjun et al., 2003; Cheng et al., 2005). The western SCS also experiences recurrent summer upwelling, under a boundary current influence with smaller MLD amplitudes (Xianjun et al., 2013).

The KC inflow into the northern SCS through Luzon Strait (Figure 1) also occurs seasonally, favored by the strong EAWM winds during winter (Xue et al., 2004; Kao et al., 2006; Liu et al., 2013). This western Pacific boundary current transports heat from low to mid-latitudes (Qiu, 2001) and impacts the northeastern SCS oceanic circulation, as it forms an anticyclonic current loop (Xue et al., 2004; Liu et al., 2013). However, this inflow branches in the SCS also affecting the west and east SCS producing cyclonic eddies (Xue et al., 2004; Liu et al., 2013). The KC intrudes into the SCS transporting large amounts of heat, which can increase this basin SSTs (Chen et al., 2003; Li et al., 2010). As the KC inflows onto the SCS, its' nutrient-enriched subsurface waters are brought to the surface upwelled by different processes, such as wind-driven upwelling, vertical mixing or cyclonic eddies (Guo et al., 2012; Chen et al., 2003, 2017).

The EAM dynamics drives PP seasonality, and latitudinal and longitudinal patterns (Su et al., 2013). In general, modern SCS has low PP, except for wind-driven upwelling areas in the western sub-basin by the EASM winds, and in the eastern sub-basin by the EAWM winds (Liu and Chai, 2009). Whereas, in the northern and southern sub-basins relatively high PP occurs during winter in response to stronger vertical mixing (deeper MLD) promoted by the strengthened EAWM NE winds (Tian et al., 2005; He et al., 2013; Su et al., 2013; Su et al., 2015).

3. Material and methods

Hole U1431D (15º22'N, 117º00'E, 4240 m water depth, 617 m of sediment recovery) was retrieved from the SCS East Sub-basin (Site U1431) (Figure 1) during the IODP Expedition 349 onboard the R/V *JOIDES Resolution*. For this study, sub-samples (N=100) of about ~10 cc were collected in 20 cm intervals from the first 20 m of the hole and archived in the Paleoceanography and Paleoclimatology Laboratory (LabPaleo²) at the Center for Marine Studies (UFPR). The sedimentation rate for this section of Hole U1431D was estimated at approximately 5 cm/ka based on onboard biostratigraphy and paleomagnetic data (Li et al., 2015).

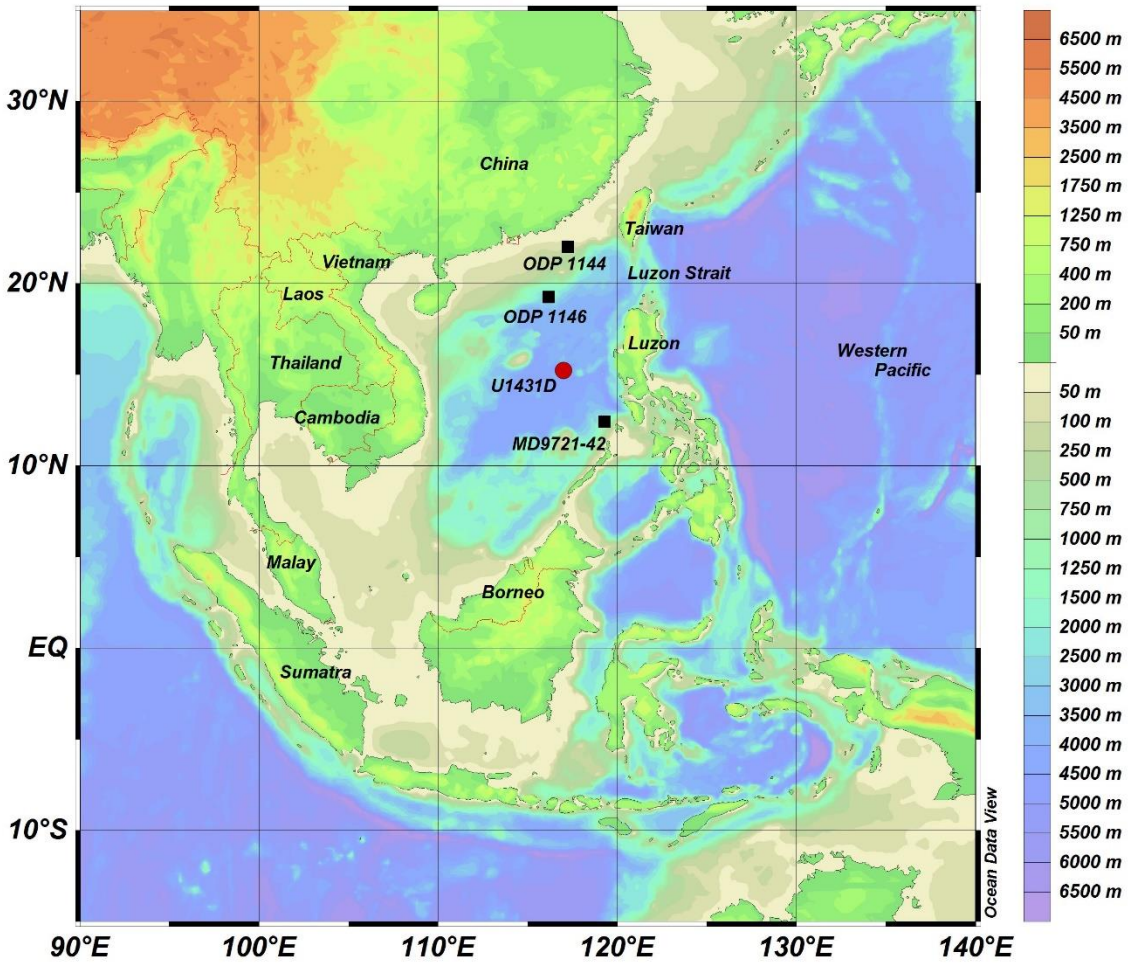

Figure 1. Study area and location of the Hole U1431D (this study) and cores MD9721-42, ODP 1144 and ODP 1146 in the South China Sea.

3.1 Chronology

A combination of oxygen isotope ($\delta^{18}O$) analysis and ^{230}Th will be performed for detailed hole chronology. The radionuclides measurements were performed in 30 samples distributed along Hole U1431D at Laboratório de Química Inorgânica Marinha (LaQIMar) from Instituto Oceanográfico (USP). The analysis was made in an EG &G ORTEC software (MAESTRO, version 6) following the methods described by Ferreira et al. (2015). ^{230}Th sedimentation rates were determined by coupled χ^2 test and Pearson correlation analysis of the nuclide behavior.

The $\delta^{18}O$ analysis will be performed in 48 samples distributed along Hole U1431D. For this, between 3 and 10, *Globigerina ruber* tests were picked from the >150 µm size fraction, species selection was made based on persistent presence in all samples. The $\delta^{18}O$ analysis will be performed using an ICP-MS at MARUM from Bremen University (Germany). The $\delta^{18}O$ curve of Hole U1431D will be tuned with the Stack LR04 chronology of Lisiecki and Raymo (2005) using the AnalySeries software (Paillard et al., 1996).

To validate the results of the unsupported ^{230}Th model, a statistical comparison will be made between its age model and the one from the planktonic foraminifera $\delta^{18}O$ record. For such, Student's t-test was used to evaluate if the two age sets are significantly similar. The t-test assumptions of data normality and homoscedasticity will be checked with Anderson–Darling and Levene tests, respectively.

3.2 Planktonic foraminifera assemblages

For this study, samples (N = 51) distributed along Hole U1431D were selected for the planktonic foraminiferal analysis. Each sample was weighed (~10g), shaken in a table for 2 hours for sediment disaggregation, washed with water in a 63 µm mesh sieve, and then oven-dried at 40°C.

To estimate the maximum planktonic foraminifera diversity in the SCS samples were dry sieved in a 150 µm mesh sieve and at least 300 specimens per sample were picked and identified under a stereo-microscope (Pflaumann and Jian, 1999; Zheng et al., 2005; Steinke et al., 2008; Yu et al., 2008). Planktonic foraminifera tests were quantified to estimate total abundance (tests/g of dry sediment). Tests were identified following the taxonomy of Parker (1962), Bé (1967), Kipp (1976) and Hemlemben et al. (1989).

Species with relative abundance averages >2% were used to perform an R-mode cluster analysis. The R-mode cluster analysis was applied to the dataset to compare the variability of the species relative abundances (Parker and Arnold, 1999).

3.3 SST Reconstruction

The SST was estimated by a transfer function applied to the planktonic foraminifera assemblages. For this, we used a Modern Analog Technique (MAT) which measures the dissimilarity index between the fauna of the fossil record and a modern fauna database from the squared chord distance where lower values represent higher similarity of the paired species. The technique is widely applied and allows the balance of the less dominant species, amplifying their signals, and abundant species (Prell, 1985; Chen et al., 2005). The fossil assemblages were compared with the data from modern SCS and Western Pacific available on MARGO (MARGO, 2004). The analysis was performed in the *software* PAST 3.0.

3.4 MLD proxy-based reconstruction

The percentage of deep-dwelling and subsurface water PF species was used as an MLD changes indicator. The abundance of these groups is depth-related according to the availability of nutrients along the water column (Jian et al., 2001; Salmon, 2015). A deeper MLD becomes the nutrient content available to the deeper layers of the water column favoring the deep-dwellers or subsurface groups (Salmon et al., 2015).

In the SCS the deep-dwellers/subsurface group are represented by *Sphaeroidinella dehiscens, Candeina nitida, Ga. praebulloides, Ga. nepenthes, Globoquadrina dehiscens, Gq. venezuelana, Pulleniatina* spp., *Neogloboquadrina* spp., *Globorotalia* spp., and *Sphaeroidinellopsis* spp. (Fairbanks et al., 1982; Li et al., 2004; Regenberg et al., 2014).

4. Results

4.1 Chronology

According to the ^{230}Th activity, the uppermost 20m of Hole U1431D comprise sediments from the Middle Pleistocene (up to MIS 8) to Present, with sedimentation rates of 7.62 cm.ka^{-1} (Figure 2). The age model will be better constrained with the results of the δ^{18}O analysis. All the samples for the δ^{18}O analysis have been picked and are waiting to be analyzed at MARUM (Bremen University/Germany), with estimated delivery of results in May 2017.

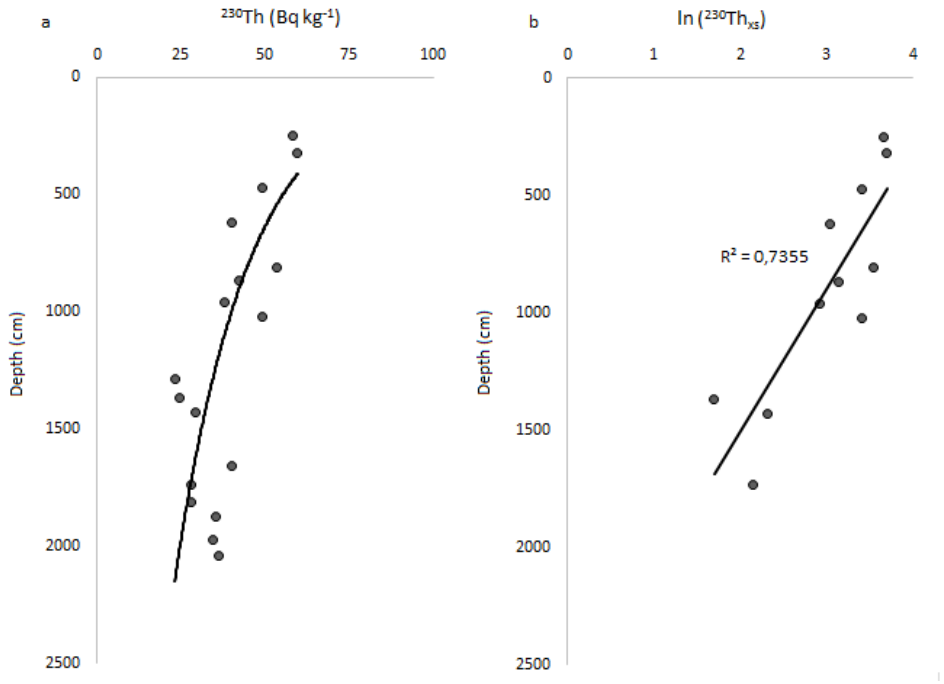

Figure 2. Vertical profile of ^{230}Th activity in a) Bq.kg^{-1} (radioactivity) and b) Linear regression obtained from core U1431D.

4.2 Planktonic foraminifera assemblages

A total of 32 species of planktonic foraminifera belonging to 13 genera were identified along the first 20 m of Hole U1431D. Species with relative abundance averages >2% represent approximately 65% of the planktonic foraminifera fauna from Hole U1431D. These include *Globigerina falconensis*, *Globoturborotalita rubescens*, *Globigerina bulloides*, *Globigerinella calida*, *Globigerinoides ruber* (white), *Globigerinoides sacculifera*, *Globorotalia menardii*, *Neogloboquadrina pachyderma* (right coiling), *Neogloboquadrina dutertrei*, *Neogloboquadrina incompta* and *Pulleniatina obliquiloculata* (Figure 3).

The R-mode cluster analysis revealed three main assemblages dominated by *P. obliquiloculata*, *G. ruber* (white) and *Ga. bulloides* (Figure 3).

The *P. obliquiloculata* assemblage is composed by *Gr. menardii* and *P. obliquiloculata* (Figure 2). Except for MIS 5, when it reaches relative abundances > 5%, this assemblage presented relatively low abundance (< 1%) throughout the record (Figure 3). The *P. obliquilocoluta* has higher relative abundance during interglacial stages, MIS 7 and MIS 5 (4.3% and 9.9%, respectively), and during the glacial stage MIS 6 (32% at approximately 146 ka). *Gr. menardii* has higher relative abundance during MIS 5 (19.2%) and MIS 3 (6%).

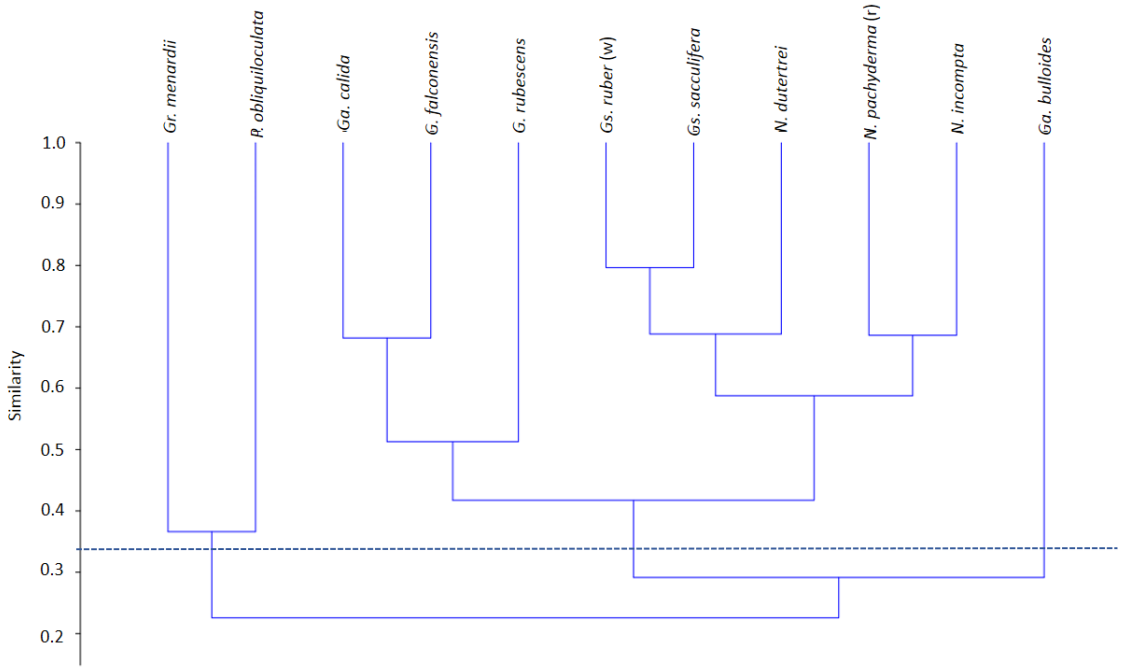

Figure 3. R-mode dendrogram for planktonic foraminifera species with relative abundance average > 2% of Hole U1431D. The similarity index derived from Euclidian distances (UPGMA method).

The *Gs. ruber* (white) assemblage can be subdivided into two subgroups, dominated by *Gs. ruber* (white) and *G. falconensis* (Figure 3). The first subgroup is composed by *Gs. ruber* (white), *Gs. sacculifera*, *N. dutertrei*, *N. pachyderma* (right coiling) and *N. incompta* (Figure 2). The species in this subgroup are the most abundant planktonic foraminifera species along U1431D record (Figure 4). *Gs. ruber* (white) and *Gs. sacculifera* represent approximately 17% and 14% of the total planktonic foraminifera fauna, respectively. In general, this subgroup occurs in higher relative abundance during interglacial stages (Figure 4). *Gs. ruber* (white), *Gs. sacculifera*, *N. dutertrei*, show relatively higher relative abundance during MIS 7, MIS 5 and MIS 3 (between 7% and 22%). While *N. pachyderma* (right coiling) and *N. incompta* show higher relative abundance during MIS 7 and MIS 3 (between 8% and 12%).

The *G. falconensis* subgroup is composed by *Ga. calida*, *G. rubescens* and *G. falconensis* (Figure 3). This subgroup species present no clear abundance distribution throughout Hole U1431D. *G. falconensis* presents relatively high abundances during MIS 8 and MIS 6 (between 7% and 17%), *G. rubescens* higher abundances occur during MIS

7, MIS 6 and MIS 3 (between 5% and 15%), and *Ga. calida* during MIS 8 (14.5%) (Figure 4).

The *Ga. bulloides* was isolated in the R-mode cluster analysis (Figure 3). This species presents overall low relative abundance with averages between 1% and 2% throughout the first 20 m of Hole U1431D, except during MIS 3 when reaches a maximum of 36.8% (Figure 4).

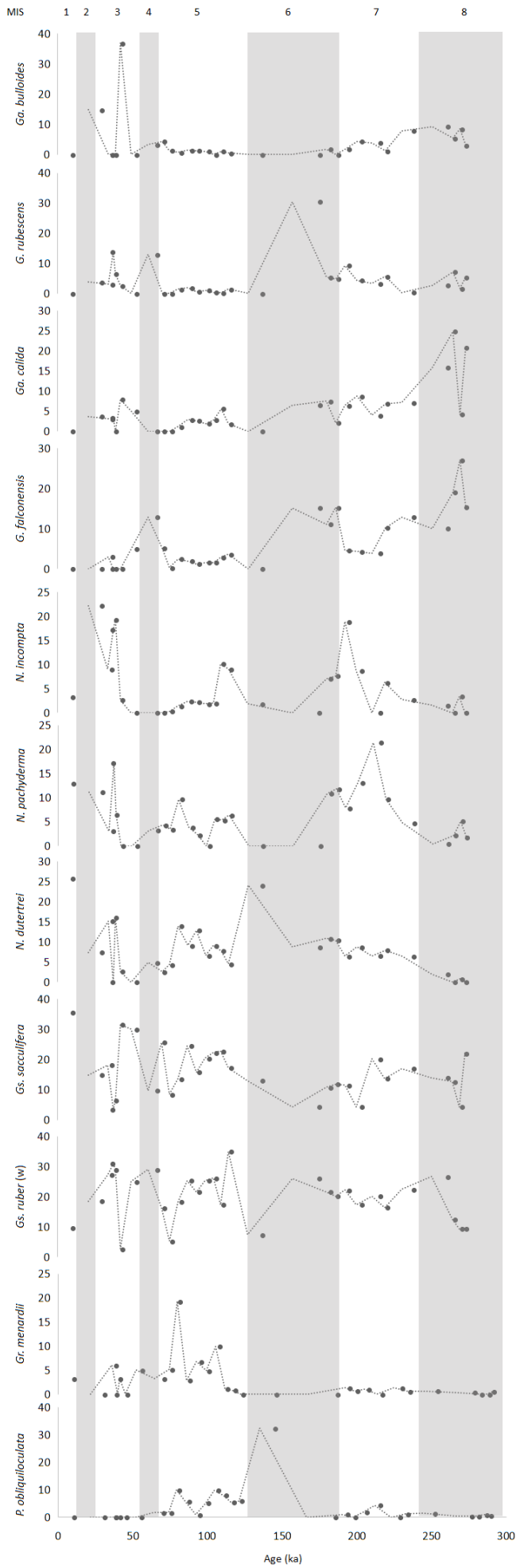

Figure 4. Along hole U1431D relative abundance of planktonic foraminifera species (>2%), *P. obliquiloculata*, *Gr. menardii*, *Gs. ruber* (white), *Gs. sacculifera*, *N. dutertrei*, *N. pachyderma* (right coiling), *N. incompta*, *G. falconensis*, *Ga. calida*, *G. rubescens*, and *Ga. bulloides*, the dotted line represents a moving 2 point average. Marine isotopic stages (MIS) are indicated by the light gray bar.

4.3 SST Reconstruction

The MAT-SST reconstruction estimated glacial SSTs ranging from 21.5°C and 25.3°C and interglacial SSTs between 26.8°C and 28.5°C (Figure 5a). In general, SSTs display higher averages (27.1°C) during interglacial stages (MIS 5 and MIS 3) and relatively lower average (26.1°C) during glacial stages (MIS 8 and MIS 6), except for one cooling event during MIS 7 (21.5°C) (Figure 5a).

4.4 MLD proxy-based reconstruction

The percentage of deep-dwelling planktonic foraminifera varied between 34.7% and 75.0% during glacial stages and from 25% to 78.5% during interglacials (Figure 5b). Higher deep-dwelling percentages are observed during MIS 8 (62.7%), MIS 6 (75.0%), MIS 5 (78.5%) while lower percentages occur during MIS 7 (48.2%) and MIS 3 (25.0%) (Figure 5b).

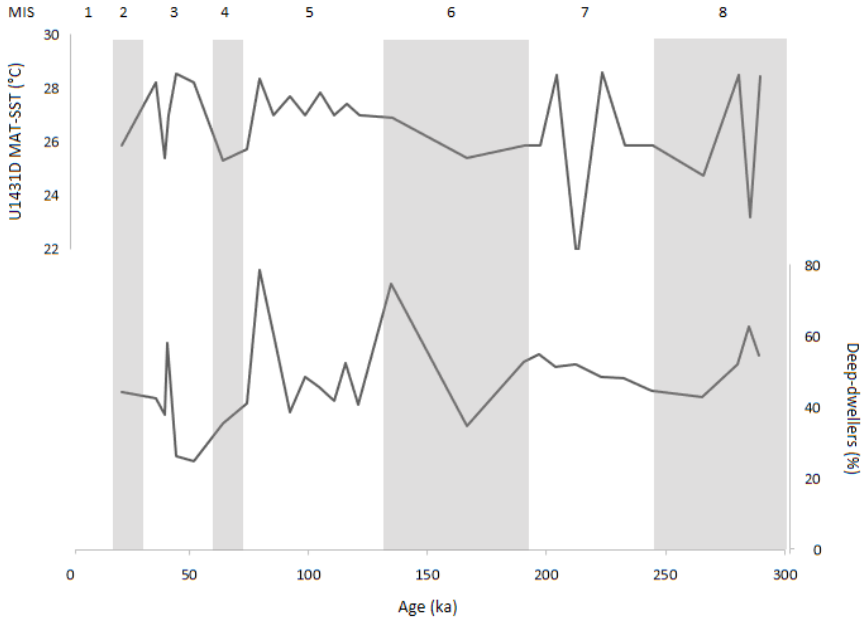

Figure 5. Along hole U1431D planktonic foraminifera (a) MAT-SST (°C) reconstruction and (b) Deep-dweller group variability. Marine isotopic stages (MIS) are indicated by the light gray bars.

5. Discussion

5.1 Planktonic foraminifera assemblage response to changes in hydrographic conditions

The planktonic foraminifera assemblages obtained in this study are commonly found in the modern SCS (e.g., Pflaumann and Jian, 1999; Lin and Hsiesh, 2007) and applied as proxies in SCS paleoceanographic reconstructions (e.g., Li et al., 2005; Xu et al., 2005; Steinke et al., 2010; Yu et al., 2013). As planktonic foraminifera assemblages respond primarily to SST and PP (Morey et al., 2005; Kucera, 2007; Jonkers and Kucera, 2015; Schiebel and Hemleben, 2016), we here discuss the East SCS sub-basin planktonic foraminifera assemblages' changes from this perspective.

The *P. obliquiloculata* assemblage is composed of tropical/subtropical species, with *P. obliquiloculata* being considered to reflect warmer modern Western Pacific conditions (Pflaumann and Jian, 1999; Zaric et al., 2005). These species are subsurface dwellers and facultative symbiont, with no clear relationship between PP and their seasonal distribution in the SCS (Pflaumann and Jian, 1999; Jonkers and Kucera, 2015). We observe increased abundances of the *P. obliquiloculata* assemblage during interglacial stages, suggesting that relatively warmer SST occupied the East portion of the SCS during these periods (Figure 4). In interglacial stages, higher abundances *Gr. menardii* and *P. obliquiloculata* in other SCS marine sedimentary records have also been related to higher SST (Andreasen and Ravelo, 1997; Jian et al., 2001; Zheng et al., 2005; Li et al., 2008).

The *Gs. ruber* (white) assemblage was subdivided into two subgroups the *Gs. ruber* (white) and *G. falconensis* (Figure 3), considered to reflect different water column conditions. The *Gs. ruber* (white) subgroup presented higher abundances during MIS 7, MIS 5 and MIS 3 while *G. falconensis* presented higher during the glacials MIS 8 and MIS 6 (Figure 3).

Typical of modern tropical and subtropical oceans the *Gs. ruber* (white) subgroup is composed of warm water and symbiont/facultative bearing species (*i.e.*, *Gs. ruber* (white), *Gs. sacculifera* and *N. dutertrei*) and by inhabitants of temperate to cold waters (*i.e., N. pachyderma* (right coiling) and *N. incompta*) (Morey et al., 2005; Jonkers and Kucera, 2015). *Gs. ruber* (white), *Gs. sacculifera* and *N. dutertrei* have their maximum abundances limited by a thermal optimum above 25 °C, responding primarily to SST conditions (Lin and Hsiesh, 2007; Jonkers and Kucera, 2015; Salmon et al., 2015). *Gs. ruber* (white) and *Gs sacculifera* are also considered to positively respond to stratified

and oligotrophic surface water conditions (Chen et al., 1998; Wang, 2000; Huang et al., 2002; Yu et al., 2006; Lin and Hsiesh, 2007; Jonkers and Kucera, 2015). Therefore, the observed high abundances of *Gs. ruber* (white) and *Gs*. *sacculifera* suggests the presence of warm and well-stratified waters during interglacial stages. Meanwhile, *N. dutertrei* has been applied in the SCS as a proxy for upwelling (Jian et al., 2001; Kuroyanagi and Kawahata, 2004; Shi et al., 2014), and high abundances (> 20%) of this species in SCS sedimentary records have been reported for the Last Glacial Maximum (LGM) and MIS 5 associated to enhanced PP (Shi et al., 2014). Additionally, in the modern SCS, the symbiont-barren *N. pachyderma* and *N. incompta* present positive correlation with high chlorophyll concentrations (Kuroyanagi and Kawahata, 2004; Jonkers and Kucera, 2015). High abundances of these species in the SCS and Pacific have also been applied as upwelling proxies (Kuroyanagi and Kawahata, 2004; Steinke et al., 2008; Yu et al., 2008). Hence, the observed high abundances of this subgroup during MIS 7, MIS 5 and MIS 3 suggests that the East SCS sub-basin experienced warm and well-stratified waters, with punctuated periods of enhanced PP.

The *G. falconensis* subgroup includes subsurface dwellers species that inhabit temperate and cold water (*i.e., G. falconensis* and *Ga. calida*) as well as surface warm tropical waters (*i.e., G. rubescens*) (Pflaumann and Jian, 1999; Peeters and Brummer, 2002; Jonkers and Kucera, 2015). Except for *G. rubescens*, this assemblage is composed of symbiont-barren species, with a close relationship and dependence of PP (Pflaumann and Jian, 1999; Jonkers and Kucera, 2015). Hence, during MIS 7 and MIS 3, higher abundances of *G. rubescens* probably reflect warmer SST in interglacials rather than changes in surface waters PP (Jonkers and Kucera, 2015). In other SCS mid-Pleistocene records *G. falconensis* and *Ga. calida* abundances present no clear glacial/interglacial patterns (Zheng et al., 2005; Yu et al., 2008). Our data, however, shows higher abundances of *G. falconensis* and *Ga. calida* during glacial stages, especially during MIS 6 and MIS 8, suggesting nutrient-enriched surface waters in this period.

Ga. *bulloides* is a surface dweller species that inhabits cold water and nutrient enriched waters (Kucera, 2007; Schiebel and Hemleben, 2016). This symbiont-barren species abundance is widely applied as an upwelling proxy (Prell and Curry, 1981; Pflaumann and Jian, 1999; Peeters and Brummer, 2002) in areas under the influence of the Indian and East Asian summer monsoon (Gupta et al., 2003; Schiebel et al., 2004; Zaric et al., 2005). Except for MIS 3 we observe overall low abundances for *Ga. bulloides* (Figure 3), which is in agreement with abundances found in modern SCS sediments

(Nathan and Leckie, 2003; Wang et al., 2014). In the northern Okinawa Trough (adjacent to the East China Sea) higher abundances of *Ga. bulloides* during MIS 3 have also been observed and related it to upwelling activity (Shi et al., 2014). Thus, *Ga. bulloides* high abundances in MIS 3 supports a scenario of higher PP at our record site during this interglacial.

Previous EAM reconstructions have shown that during interglacial (glacial) stages strengthened EASM (EAWM) promotes warm and humid (cold and dry) climatic conditions over the Asian continent (Guo et al., 2008 *and references therein*). The enhanced precipitation from the EASM would lead to a decrease in SCS surface waters salinity and density (Duan et al., 2012) resulting in a well-stratified water column. This scenario supports the presence of warm and oligotrophic surface waters in the East SCS sub-basin inferred from the predominance of *P. obliquiloculata* and *Gs. ruber* (white) assemblages during late Quaternary interglacial stages.

Our PF record, however, is also marked by periods with high abundances of species considered to inhabit high PP waters (i.e., *N. dutertrei*, N. *pachyderma*, *N. incompta*, *Ga. bulloides*, *Ga. calida* and *G. falconensis*). Thus, suggesting that during interglacial stages MIS 7, 5, and 3, and glacial MIS 8 the East SCS sub-basin surface waters experienced periods of increased PP. The EAM seasonal dynamics (EAWM and EASM) drive modern SCS PP, impacting each of the SCS sub-basins superficial circulation (Liu et al., 2002; Hess and Khunt, 2005; Su et al.; 2013; Shi et al., 2014) differently. This is reflected in SCS PP reconstructions, as previous studies have suggested that during glacial stages the EAWM controlled PP in the northern SCS (e.g., He et al., 2013); while there is no consensus for PP patterns and driving mechanisms over the rest of the SCS (e.g., Wei et al., 2003; Wang et al., 2007).

The EAM seasonal dynamics (EAWM and EASM) drive modern SCS PP, impacting each of the SCS sub-basins superficial circulation differently (Liu et al., 2002; Hess and Khunt, 2005; Su et al.; 2013; Shi et al., 2014). For the East SCS sub-basin, where our site is located, PP devoid a clear seasonal pattern, being primarily controlled by wind-driven Ekman convergence/divergence (upwelling/downwelling) rather than by wind-driven vertical mixing (Siswanto et al., 2017). During glacial stages, MIS 6 and MIS 8 relatively high abundances of the symbiont-barren *Ga. calida* and *G. falconensis* observed in Hole U1431D point to nutrient enriched surface waters. High abundances of *G. falconensis* have been considered to be a reliable proxy for strong EAWM as its high abundances in the Arabian Sea reflect high PP waters during non-upwelling conditions

(Peeters and Brummer, 2002; Schultz et al., 2002). Hence, in these glacial stages, we propose that a strengthened EAWM (Hao et al., 2012) would act as an effective upper-ocean mixing agent and supply nutrients to the surface waters enhancing PP.

Conversely, during late Quaternary interglacial stages, with a weak EAWM (Hao et al., 2012), surface water nutrient supply would have resulted from other driving mechanisms. Interglacial stages are marked by (i) strengthened EASM and (ii) high relative sea level conditions (Figure 6b,f). The first enhances PP in the East SCS sub basin through wind-driven upwelling of deeper nutrient-enriched waters, while the later, allows a more efficient KC inflow through the Luzon Strait (Xu et al., 2005; Liu et al., 2013; Shi et al., 2014; Li et al., 2017), enabling PP increase (Chen et al., 2001; Liu et al., 2013).

For the interglacial MIS 7 and MIS 3, we observe relatively high abundances of *N. dutertrei*, *N. pachyderma*, *N. incompta*, *Ga. bulloides* commonly applied as upwelling proxies (Jian et al., 2001; Kuroyanagi and Kawahata, 2004; Yu et al., 2008; Shi et al., 2014). These species suggest that during these interglacials strong EASM winds promoted upwelling of nutrient-enriched waters and PP enhancement in the East SCS (Figure 6.b). Specifically, for MIS 5, it is possible that strong EASM winds and KC inflow, due to elevated relative mean sea level, contributed to PP enhancement. Other studies have proposed the exchange of waters between the SCS and the Pacific Ocean, through the KC inflow, as the primary factor affecting PP increase during this interglacial stage (Li et al., 2010; He et al., 2013). MIS 5 features the highest relative mean sea level in the last 300 ka (approximately 9 to 13 m above the Present, Figure 5.f) (Bates et al., 2014). As a consequence of the warm KC intrusion waters in MIS 5, high *P. obliquiloculata*/*N. pachyderma* ratio is observed (Figure 6g). Therefore, in this interglacial, the East SCS sub-basin hydrodynamic and PP were under the large KC influence.

Our results suggest that in the last 300 ka interglacial stages, the East SCS sub-basin waters were dominated by typical tropical and subtropical planktonic foraminifera species (*P. obliquiloculata, Gr. menardii, Gs. ruber* (white), *Gs. sacculifera, N. dutertrei, G. rubescens*), inhabiting warm and oligotrophic waters promoted by a strengthened EASM, while, as secondary components of the fauna, temperate to cold water species (*G. falconensis, Ga. calida, N. pachyderma, N. incompta* and *Ga. bulloides*) are present during specific interglacial and glacial stages intervals in response to punctuated enhanced PP. In these periods increased PP, the physical processes (*i.e.*, wind-driven upwelling and upper-ocean mixing) driven by the EAM winds, and the KC inflow, under

high relative mean sea level, may have played a significant role in the East SCS sub-basin surface waters environmental conditions.

5.2 East SCS sub-basin planktonic foraminifera based SST and MLD reconstructions

PF based transfer function techniques are widely applied in paleoceanography studies independent of location (e.g., Kucera et al., 2005; Chapori et al., 2015; Haddam et al., 2016). However, in the SCS, this method has rarely been applied since a no-analogue situation was reported by Steinke et al. (2008). According to these authors, in the Last Glacial Maximum (LGM), anomalous high percentages of *P. obliquiloculata* and *N. pachyderma* (the warmest and coldest fauna, respectively, of the Western Pacific) observed in SCS records would invalidate the application of PF based transfer function for SST reconstructions during this cold event. Our MAT-SST reconstruction suggests that the East SCS sub-basin experienced SST fluctuations of approximately 1°C on average between glacial and interglacial stages over the past 300 ka (Figure 6e). The *P. obliquiloculata*/*N. pachyderma* ratio is higher only during the interglacial MIS 5. Thus, we refuse a no-analogue situation in our glacial SST reconstructions. Additionally, our SST estimates for glacial and interglacial stages are in accordance with previously published SST curves based both on planktonic foraminifera transfer function (Chen et al., 2003), and Mg/Ca based SST (Wei et al., 2007), from the east and north SCS sub-basins, respectively (Figure 6c and 6d).

Meanwhile, for the interglacial stages, the *P. obliquiloculata*/*N. pachyderma* ratio can be applied as a proxy for warm subsurface waters in the SCS in response to the inflow of warm waters from Western Pacific in the SCS (Li et al., 2004). The late Quaternary relationship between SST and the KC inflow has been suggested by Chen et al. (2003). These authors found significant SST fluctuations and glacial/interglacial patterns, with amplitudes of 1.8-3.5°C in the SCS (Figure 6d). According to these authors, during the glacial and interglacial stages, the inflow of these warm waters was controlled by the exposure of the connections with open oceans with changing sea level. Sea-level oscillations, and the consequent KC inflow to the SCS are not the only mechanism behind SCS SST changes (e.g., Cheng et al., 2005; Wei et al., 2007).

Modern SCS presents a north-south SSTs latitudinal gradient with increasing SST from north to south, controlled by the intensity of the EAM (Cheng et al., 2005). This gradient is present in the SSTs reconstruction over the last 300 ka, as reconstructed SST

in the north sub-basin (core 1144, Wei et al., 2007) are lower than those found in the eastern sub-basin (U1431D, this study), which in turn are lower than those observed for a core located further south (MD97-2142, Chen et al., 2003) (Figure 6). Our SST reconstruction presents similar patterns with both the EAM and sea level records (Figure 6). Our temporal resolution, however, does not allow for a better constraint of the controlling mechanism behind the SCS eastern sub-basin SST changes in the late Quaternary.

The EAM and SST changes also influence latitudinal and longitudinal variations in the MLD of the SCS (Qu, 2001; Xianjun et al., 2013). In the East sub-basin, MLD is mainly controlled by the overlying atmosphere temperatures and EAM wind stress are less important (Xianjun et al., 2003; Cheng et al., 2005). Hence, during glacial (interglacial) stages negative (positive) heat flux would favor a deeper (shallower) MLD in the eastern SCS sub-basin. Our MLD reconstruction based on the deep-dwelling PF, is in agreement with this, as it reveals deeper MLD during glacial stages (MIS 8 and MIS 6) (Figure 6i). However, there is no clear contrast between glacial and interglacial stages, as during interglacial stages MIS 7 and MIS 5 deep-dwelling PF percentages are also relatively high (Figure 6i). Which suggests that either (i) air-sea heat flux was not the main controlling factor for the late Quaternary eastern sub-basin MLD patterns or (ii) deep-dwelling PF percentages is not a good proxy to infer MLD in the East SCS sub-basin.

We favor the latter as according to fauna and Mg/Ca based SST reconstructions, during interglacial stages warmer SST predominated in the SCS (Figure 6), this would promote a more stable water column, leading to shallower MLD. In general, deep-dwelling PF text flux to the seafloor positively responds to enhanced primary productivity related to deeper MLD (Salmon et al., 2015). In fact, our deep-dwelling PF respond to PP as shown by similar patterns with other paleoproductivity proxies (Ba/Sc ratio) from northern SCS (Figure 6h) (Wan et al., 2010). However, in the SCS the nutrient supply, resulting in enhanced PP, can be promoted by vertical mixing, upwelling activity or changes in the circulation from exchange waters of Western Pacific (He et al., 2013), as shown in our data. These physical processes affect the upper-ocean thermal structure in different and complex ways (Jian et al., 2001; He et al., 2013), which does not translate to the correlation between deeper (shallower) MLD and increased (decreased) PP.

Our data suggests that in the last 300 ka the East SCS sub-basin surface water conditions (*i.e.*, SST and PP) were influenced by the EAM and the KC inflow. The latter

has been particularly significant during interglacial stages, under high relative mean sea level. The interglacial stages featured surface waters predominantly warm, oligotrophic, and well stratified, in response to the EASM, but have been punctuated at times with enhanced PP, in response to changes in nutrient supply by wind-driven upwelling and the KC inflow. Meanwhile, glacial stages were characterized by the presence of cold and nutrient enriched waters, with a relatively less stratified water column, related to vigorous vertical mixing in response to the strong EAWM wind.

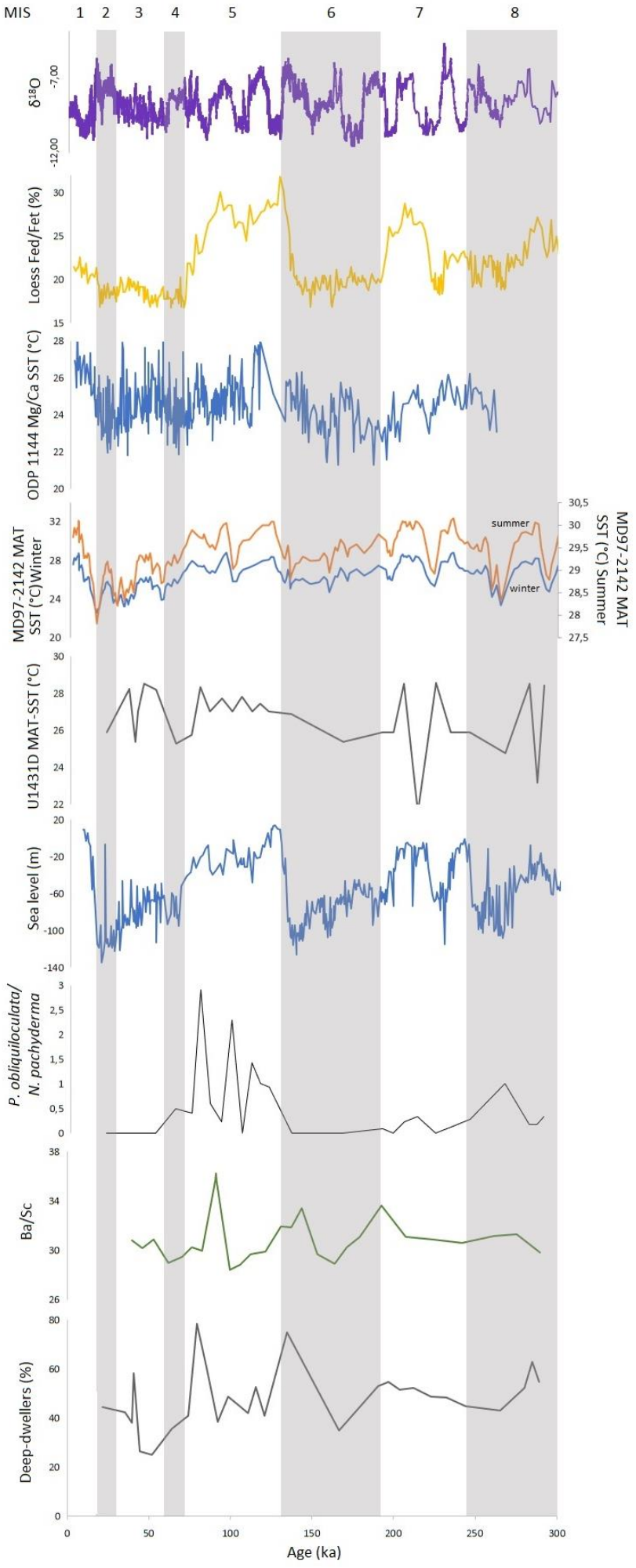

Figure 6. South China Sea proxies compared to continental EAM records and sea level. (a) EAM variations from Dongge and Hulu Cave $\delta^{18}O$ (Wang et al., 2008); (b) Redness from Xifeng loess (chemical weathering) (Guo et al., 2008); (c) *Gs. sacculifera* Mg/Ca ratios-based SST from ODP 1144 (northern SCS) (Wei et al., 2007); (d) MAT PF-based SST from MD97-2142 for cold and warm season (east SCS) (Chen et al., 2003); (e) MAT-based MLD from U1431D (this study); (f) Relative sea level from ODP site 181-1123 (Pacific) (Bates et al., 2014); (g) *P. obliquiloculata*/*N. pachyderma* ratio from U1431D (this study); (h) Ba/Sc from ODP 1146 site (northern SCS) (Wan et al., 2010); and (i) Deep-dweller group percentage from U1431D (this study).

6. Conclusions

In the last 300 ka, planktonic foraminifera assemblages from East SCS sub-basin (Hole U1431D) reflect changes in SST and PP conditions. We interpreted these changes as responses to the EAM dynamics and the KC inflow into the SCS. Our data allowed us to infer that EASM winds favored the presence of warm, oligotrophic, and well-stratified surface waters in the East SCS sub-basin during interglacial stages; with episodic enhanced PP, as the KC inflow brought nutrient enriched waters from the Pacific Ocean. As a response to a strengthened EAWM, cold and productive surface waters occupied the East SCS sub-basin during glacial stages. Our data also highlights that the East SCS sub-basin has a complex hydrodynamic response to Late Quaternary glacial and interglacial cycles. As the upper-ocean in this part of the SCS responds to both ocean-atmosphere interactions (EAM dynamics) and sea level oscillations (KC inflow). East SCS sub-basin appear to have a great potential to aid in the understanding of the exchange of waters between the SCS and the Western Pacific and it's the implications, especially during higher sea-level events.

Acknowledgements

This research is based on samples and data collected by the International Ocean Discovery Program (IODP). The science party members, crew, and technicians aboard the R/V JOIDES Resolution are acknowledged for their work during IODP Expedition 349. Funding was provided by IODP/CAPES-Brasil (Edital 38/2014), and Fundação de Amparo à Pesquisa do Estado de São Paulo (FAPESP; Proc. n°.2015/11832-2). The authors would also like to acknowledge CAPES for scholarships received by Renata Hanae Nagai (BEX 14531/13-5) and Amanda Gerotto (Demanda Social).

References

Andreasen, D.J. and Ravelo, A.C. 1997. Tropical Pacific Ocean thermocline reconstructions for the last glacial maximum. *Paleoceanography*, 12, 395–413.

Bé, A.W.H.. 1967. Foraminifera, families: Globigerinidae and Globor- otaliidae. In: Fraser, J.H. (Ed.), Fiches d'Indentification du Zooplancton,Cons. Int.Explor.Mer,Charlottenlund, Sheet.

Chen, C., Jan, S., Kuo, T. and Li, S. 2017. Nutrient fl ux and transport by the Kuroshio east of Taiwan. *Journal of Marine Systems*, 167, 43–54.

Chen, M.-T, Huang, C.C., Pflaumann, U., Waelbroeck, C. and Kucera, M. 2005. Estimating Glacial Western Pacific Sea-Surface Temperature: Methodological Overview and Data Compilation of Surface Sediment Planktic Foraminifer Faunas. *Quaternary Science Reviews*, 24, 1049–62.

Chen, M.-T., Ho, H.-W., Lai, T.-D., Zheng, L., Miao, Q., Shea, K.-S., … Huang, C.-Y. 1998. Recent planktonic foraminifers and their relationships to surface ocean hydrography of the South China Sea. *Marine Geology*, 146, 173–190.

Chen, M.-T., Shiau, L.-J., Yu, P.-S., Chiu, T.-C., Chen, Y.-G. and Wei, K.-Y. 2003. 500 000-Year records of carbonate, organic carbon, and foraminiferal sea-surface temperature from the southeastern South China Sea (near Palawan Island). *Palaeogeography, Palaeoclimatology, Palaeoecology*, 197, 113–131.

Chen, M.-T., Wang, P., Wang, L., Sarnthein, M., Wang, C.H. and Huang, C.Y. 1999. A late Quaternary planktonic foraminifer faunal record of rapid climatic changes from the South China Sea. *Marine Geology*, 156, 85–108.

Chen, M.-T.A., Wang, S.-L., Chou, W.-C. and Sheu, D.D. 2006. Carbonate chemistry and projected future changes in pH and CaCO3 saturation state of the South China Sea. *Marine Chemistry*, 101, 277–305.

Cheng, H., Sinha, A., Wang, X., Cruz, F. and Edwards, R.L. 2012. The Global Paleomonsoon as seen through speleothem records from Asia and the Americas. *Climate Dynamics*, 39, 1045–1062.

Cheng, X., Huang, B., Jian, Z., Zhao, Q., Tian, J. and Li, J. 2005. Foraminiferal isotopic evidence for monsoonal activity in the South China Sea: A present-LGM comparison. *Marine Micropaleontology*, 54, 125–139.

Dong, L., Li, L., Li, Q., Wang, H. and Zhang, C. L. 2015. Hydroclimate implications of thermocline variability in the southern South China Sea over the past 180,000yr. *Quaternary Research (United States)*, 83, 370–377.

Duan, R., Yang, K., Ma, Y. and Hu, T. 2012. A Study of the Mixed Layer of the South China Sea Based on the Multiple Linear Regression. *Acta Oceanologica Sinica*, 31, 19–31.

Fairbanks, R.G., Sverdlove, M., Free, R., Wiebe, P.H. and Bé, A.W.H. 1982. Vertical distribution and isotopic fractionation of living planktonic foraminifera from the Panama Basin. *Nature*, 298, 841–844.

Ferreira, P.A.L., Costa, K.B., Toledo, F.A.L. and Figueira, R.C.L. 2015. Sedimentation rates and age modeling of Late Quaternaty marine sediments with unsupported 230Th. *Journal of Radioanalytical and Nuclear Chemistry*, 304, 829-836.

Guo, X., Zhu, X., Wu, Q. and Huang, D. 2012. The Kuroshio nutrient stream and its temporal variation in the East China Sea. *Journal Of Geophysical Research*, 117, 1-17.

Guo, Z.T., Berger, a., Yin, Q.Z. and Qin, L. 2008. Strong asymmetry of hemispheric climates during MIS-13 inferred from correlating China loess and Antarctica ice records. *Climate of the Past Discussions*, 4, 1061–1088.

Gupta, A.K., Anderson, D.M. and Overpeck, J.T. 2003. Abrupt changes in the Asian southwest monsoon during the Holocene and their links to the North Atlantic Ocean. *Nature*, 421, 4–7.

He, Z. and Wu, R. 2013. Coupled Seasonal Variability in the South China Sea. *Journal of Oceanography*, 69, 57–69.

Hemleben, C., Spindler, M. and Anderson, O.R., 1989. Modern Planktonic Foraminifera. Springer, New York.

Hess, S. and Kuhnt, W. 2005. Neogene and Quaternary Paleoceanographic Changes in the Southern South China Sea (Site 1143): The Benthic Foraminiferal Record. *Marine Micropaleontology*, 54, 63–87.

Jian, Z., Huang, B., Kuhnt, W. and Lin, H.L. 2001. Late Quaternary Upwelling Intensity and East Asian Monsoon Forcing in the South China Sea. *Quaternary Research*, 55, 363–70.

Jonkers, L., and Kučera, M. 2015. Global analysis of seasonality in the shell flux of extant planktonic Foraminifera. *Biogeosciences*, 12, 2207–2226.

Kao, S.J., Wu, C., Hsin, Y. and Dai, M. 2006. Effects of sea level change on the upstream Kuroshio Current through the Okinawa Trough. *Geophysical Research Letters,* 33, 1–5.

Kucera, M. 2007. Chapter Six Planktonic Foraminifera as Tracers of Past Oceanic Environments, 1, 213–262.

Kuroyanagi, A. and Kawahata, H. 2004. Vertical distribution of living planktonic foraminifera in the seas around Japan. *Marine Micropaleontology*, 53, 173–196.

Li, B., Jian, Z., Li, Q., Tian, J. and Wang, P. 2005. Paleoceanography of the South China Sea since the middle Miocene: Evidence from planktonic foraminifera. *Marine Micropaleontology*, 54, 49–62.

Li, B., Wang, J., Huang, B., Li, Q., Jian, Z., Zhao, Q., Su, X. and Wang P. 2004. Correction to "South China Sea surface water evolution over the last 12 Myr: A south-north comparison from Ocean Drilling Program Sites 1143 and 1146." *Paleoceanography*, 19, 1–12.

Li, C.-F., Lin, J., Kulhanek, D.K., Williams, T., Bao, R., Briais, a., … Zhao, X. 2015. Site U1431. In Li, C.-F., Lin, J., Kulhanek, D.K. and the Expedition 349 Scientists, *Proceedings of the International Ocean Discovery Program, 349: South China Sea Tectonics*: *College Station*, TX (International Ocean Discovery Program).

Li, D., Chiang, T., Kao, S., Hsin, Y., Zheng, L., Yang, J.T., … Dai, M. 2017. Journal of Asian Earth Sciences Circulation and oxygenation of the glacial South China Sea. *Journal of Asian Earth Sciences*, 138, 387–398.

Li, Q., Wang, P., Zhao, Q., Tian, J., Cheng, X., Jian, Z., Zhong, G. and Chen, M. 2008. Paleoceanography of the Mid-Pleistocene South China Sea. *Quaternary Science Reviews* 27, 1217–33.

Li, T., Zhao, J., Sun, R., Chang, F. and Sun, H. 2010. Marine Micropaleontology The variation of upper ocean structure and paleoproductivity in the Kuroshio source region during the last 200 kyr. *Marine Micropaleontology*, 75(1-4), 50–61.

Lin, H.-L. and Hsieh, H.-Y. 2007. Seasonal variations of modern planktonic foraminifera in the South China Sea. *Deep Sea Research Part II: Topical Studies in Oceanography*, 54(14-15), 1634–1644

Lisiecki, L.E. and Raymo, M.E. 2005. A Pliocene-Pleistocene stack of 57 globally distributed benthic δ^{18}O records. *Paleoceanography*, 20(1), n/a–n/a.

Liu, G. and Chai, F. 2009. Seasonal and interannual variability of primary and export production in the South China Sea : a three-dimensional physical – biogeochemical model study, *International Council for the Exploration of the Sea*, 420–431.

Liu, J., Li, T., Xiang, R., Chen, M., Yan, W., Chen, Z. and Liu, F. 2013. Influence of the Kuroshio Current intrusion on Holocene environmental transformation in the South China Sea. *The Holocene*, 23, 850-859.

Liu, K., Chao, S., Shaw, P., Gong, G., Chen, C. and Tang, T.Y. 2002. Monsoon-forced chlorophyll distribution and primary production in the South China Sea : observations and a numerical study. *Deep-Sea Research, 49*, 1387–1412.

Liu, Q., Kaneko, A. and Su, J. 2008. Recent Progress in Studies of the South China Sea Circulation. *Journal of oceanography*, 64, 753–62.

Liu, Z., Colin, C., Li, X., Zhao, Y., Tuo, S., Chen, Z., … Huang, K.-F. 2010. Clay mineral distribution in surface sediments of the northeastern South China Sea and surrounding fluvial drainage basins: Source and transport. *Marine Geology*, 277, 48–60.

MARGO, 2004. MARGO Multiproxy Approach for the Reconstruction of the Glacial Ocean surface (archived project web pages and templates), Bremerhaven, PANGAEA .

McClymont, E. L., Sosdian, S. M., Rosell-Melé, A. and Rosenthal, Y. 2013. Pleistocene Sea-Surface Temperature Evolution: Early Cooling, Delayed Glacial Intensification, and Implications for the Mid-Pleistocene Climate Transition. *Earth-Science Reviews* 123, 173–93.

Morey, A.E., Mix, A.C. and Pisias, N.G. 2005. Planktonic foraminiferal assemblages preserved in surface sediments correspond to multiple environment variables. *Quaternary Science Reviews*, 24, 925–950.

Nathan, S.A. and Leckie, R. 2003. Miocene planktonic foaminiferal biostratigraphy of Sites 1143 and 1146, ODP Leg 184, South China Sea. *In: Prell, WL; Wang, P; Blum, P; Rea, DK; Clemens, SC (eds.) Proceedings of the Ocean Drilling Program, Scientific Results, College Station, TX (Ocean Drilling Program)*, 184, 1-43.

Paillard, D., Labeyrie, L. and Yiou, P. 1996. AnalySeries 1.0: a Macintosh software for the analysis of geophysical time-series. *Eos Transactions*, AGU, 77, pp. 379.

Parker, F.L. 1962. Planktonic foraminiferal species in Pacific sediments, Micropaleontology, 8, 219-254.

Parker, W.C. and Arnold, A.J. Quantitative methods of data analysis in foraminiferal ecology. 1999. In: Gupta, B.K.S. *Modern Foraminifera*. Published by Kluwer Academic Publishers, Grain Bretain. pp. 71-89.

Peeters, F.J.C., Brummer, G.-J.A. and Ganssen, G.M. 2002. The effect of upwelling on the distribution and stable isotope composition of *Globigerina bulloides* and *Globigerinoides ruber* (planktic foraminifera) in modern surface waters of the NW Arabian Sea. *Global and Planetary Change*, 34, 269–291.

Pflaumann, U. and Jian, Z. 1999. Modern Distribution Patterns of Planktonic Foraminifera in the South China Sea and Western Pacific : A New Transfer Technique to Estimate Regional Sea-Surface Temperatures. *Marine Geology*, 156, 41–83.

Prell, W.L. and Curry, W.B. 1981. Faunal and isotope indices of monsoonal upwelling: Western Arabia Sea. *Oceanologica Acta*, 4, 91–98.

Qu, T. 2001. Role of ocean dynamics in determining the mean seasonal cycle of the South China Sea surface temperature. *Journal Of Geophysical Research*, 106, 6943–6955.

Regenberg, M., Regenberg, A., Garbe-Schonberg, D., Lea, D.W. 2014. Global Dissolution Effects on Planktonic Foraminiferal Mg/Ca Ratios Controlled by the Calcite-Saturation State of Bottom Waters. *Paleoceanography*, 29, 127–42.

Ren, H., Sigman, D.M., Chen, M. and Kao, S. 2012. Elevated foraminifera-bound nitrogen isotopic composition during the last ice age in the South China Sea and its global and regional implications. *Global Biogechemical Cycles*, 26, 1–13.

Salmon, K.H., Anand, P., Sexton, P.F. and Conte, M. 2015. Upper Ocean Mixing Controls the Seasonality of Planktonic Foraminifer Fluxes and Associated Strength of the Carbonate Pump in the Oligotrophic North Atlantic. *Biogeosciences*, 12, 223–35.

Schiebel, R. 2002. Planktic foraminiferal sedimentation and the marine calcite budget. *Global Biogeochemical Cycles*, 16, 3-1-3-21.

Schiebel, R. and Hemleben. 2016. Planktic Foraminifers in the Modern Ocean: Ecology, Biogeochemistry, and Application. Springer. ISBN 3662502976, 9783662502976, pp. 333.

Schiebel, R., Zeltner, A., Treppke, U.F., Waniek, J.J., Bollmann, J., Rixen, T. and Hemleben, C. 2004. Distribution of diatoms, coccolithophores and planktic

foraminifers along a trophic gradient during SW monsoon in the Arabian Sea. *Marine Micropaleontology*, 51, 345–371.

Shi, X., Wu, Y., Zou, J., Liu, Y., Ge, S., Zhao, M., … Han, Y. 2014. Multiproxy reconstruction for Kuroshio responses to northern hemispheric oceanic climate and the Asian Monsoon since Marine. *Climate of the Past*, 10, 1735–1750.

Steinke, S., Kienast, M., Pflaumann, U., Weinelt, M., Stattegger, K. 2001. A High-Resolution Sea-Surface Temperature Record from the Tropical South China Sea (16,500–3000 Yr B.P.). *Quaternary Research*, 55, 352–62.

Steinke, S., Chiu, H.Y., Yu, P-S., Shen, C.C., Erlenkeuser, H., Löwemark., L. and Chen, M.T. 2006. "On the Influence of Sea Level and Monsoon Climate on the Southern South China Sea Freshwater Budget over the Last 22,000 Years." *Quaternary Science Reviews*, 25, 1475–88.

Steinke, S., Mohtadi, M., Groeneveld, J., Lin, L.C., Löwemark., L, Chen, M.T. and Rendle-Bühring, R. 2010. Reconstructing the Southern South China Sea Upper Water Column Structure since the Last Glacial Maximum : Implications for the East Asian Winter Monsoon Development. *Paleoceanography*, 25, 1–15.

Steinke, S., Yu, P-S., Kucera, M. and Chen M.T. 2008. No-Analog Planktonic Foraminiferal Faunas in the Glacial Southern South China Sea : Implications for the Magnitude of Glacial Cooling in the Western Pacific Warm Pool. *Marine Micropaleontology*, 66: 71–90.

Su, X., Liu, C., Beaufort, L., Barbarin, N. and Jian, Z. 2015. Differences in Late Quaternary primary productivity between the western tropical Pacific and the South China Sea: Evidence from coccoliths. *Deep-Sea Research Part II: Topical Studies in Oceanography*, 122, 131–141.

Su, X., Liu, C., Beaufort, L., Tian, J. and Huang, E. 2013. Late Quaternary coccolith records in the South China Sea and East Asian monsoon dynamics. *Global and Planetary Change*, 111, 88–96.

Tian, J., Wang, P.X., Chen, R.H. and Cheng, X.R. 2005. Quaternary Upper Ocean Thermal Gradient Variations in the South China Sea: Implications for East Asian Monsoon Climate. *Paleoceanography*, 20, 1-8.

Tian, J., Huang, E. and Pak, D. 2010. East Asian winter monsoon variability over the last glacial cycle: insights from a latitudinal sea-surface temperature gradient across the South China Sea. *Palaeogeography, Palaeoclimatology, Palaeoecology*. 292, 319–324.

Wan, S.M., Li, A.C., Clift, P. D., Wu, S.G., Xu, K.H. and Li, T.G. 2010. Increased contribution of terrigenous supply from Taiwan to the northern South China Sea since 3 Ma. *Marine Geology*, 278, 115–121.

Wang, B. and Ding, Q. 2008. Global monsoon: dominant mode of annual variation in the tropics. *Dynamics of Atmospheres and Oceans* 44:165–183

Wang, L., Sarnthein, M., Erlenkeuser, H., Grimalt, J.O., Grootes, P., Heilig, S., … Pflaumann, U. 1999. East Asian monsoon climate during the latePleistocene: High-resolution sediment records from the South China Sea. *Marine Geology*, 156, 243–282

Wang, P., Li, Q. and Tian, J. 2014. Pleistocene paleoceanography of the South China Sea: Progress over the past 20 years. *Marine Geology*, 352, 381–396.

Wang, R. J., Jian, Z.M., Xiao, W.S., Tian, J., Li, J.R., Chen, R.H., Zheng, Y.L. and Chen, J.F. 2007. Quaternary biogenic opal records in the South China Sea: Linkages to East Asian monsoon, global ice volume and orbital forcing. S*cience in China Series D: Earth Sciences*, 50, 710–724.

Wang, P. and Q. Li., 2009. Oceanographical and geological background, in The South China Sea, Development in Paleoenvironmental Research, vol. 13, edited by P. Wang and Q. Li, pp. 25–73, Springer Science+Business Media B.V., Netherlands

Wang, Y., Cheng, H., Edwards, R.L., Kong, X., Shao, X., Chen, S., … An, Z. Millennial- and orbital- scale changes in the East Asian Monsoon over the past 224,000 years. *Nature*, 451, 1090–1093.

Wefer, G., Berger, W.H., Bijma, J. and Fisher, G.1999. Clues to ocean history: A brief overview of proxies. In: Fisher, G. and Wefer, G. eds.. Use of proxies in paleoceanography: Examples from South Atlantic. Springer-Verlag, Berlin, Heidelberg.

Wei, G., Deng, W., Liu, Y. and Li, X. 2007. High-resolution sea surface temperature records derived from foraminiferal Mg / Ca ratios during the last 260 ka in the northern South China Sea. *Palaeogeography, Palaeoclimatology, Palaeoecology*, 250, 126–138.

Wei, K., Chiu, T. and Chen, Y. 2003. Toward establishing a maritime proxy record of the East Asian summer monsoons for the late Quaternary. *Marine Geology,* 201, 67–79.

Xianjun, X., Dongxiao, W., Wen, Z., Zuqiang, Z., Yinghao, Q.I.N., Na, H.E. and Lili, Z. 2013. Impacts of a Wind Stress and a Buoyancy Flux on the Seasonal Variation of Mixing Layer Depth in the South China Sea. *Acta Oceanologica Sinica,* 32, 30–37.

Xu, J., Wang, P., Huang, B., Li, Q. and Jian, Z. 2005. Response of planktonic foraminifera to glacial cycles: Mid-Pleistocene change in the southern South China Sea. *Marine Micropaleontology*, 54, 89–105.

Xue, H. J., Chai, F., Pettigrew, N., Xu, D.Y., Shi, M. and Xu, J. P. 2004. Kuroshio intrusion and the circulation in the South China Sea. *Journal of Geophysical Research-Ocea*ns, 109, C2.

Yu, P-S. and Chen, M-T. 2013. Millennial-to-Orbital Scale Changes in the Planktic Foraminiferal Assemblages and Sea Surface Temperature in the South China Sea during the Past 135 Kya. *Geophysical Research Abstracts,* 15, 9190.

Yu, P-S., Huang, C., Chin, Y., Mii, H., and Chen, M. 2006. Late Quaternary East Asian Monsoon variability in the South China Sea : Evidence from planktonic foraminifera faunal and hydrographic gradient records, *236*, 74–90.

Yu, P-S., Mii, H. S., Murayama, M. and Chen, M-T. 2008. Late Quaternary Planktic Foraminifer Fauna and Monsoon Upwelling Records from the Western South China Sea, near the Vietnam Margin (IMAGES MD012394). *Terrestrial, Atmospheric and Oceanic Sciences* 19, 347–62.

Zaric, S., Donner, B., Fischer, G., Mulitza, S. and Wefer, G. 2005. Sensitivity of planktic foraminifera to sea surface temperature and export production as derived from sediment trap data. *Marine Micropaleontology,* 55, 75–105.

Zheng, F., Li, Q., Li, B., Chen, M., Tu, X., Tian, J. and Jian, Z. 2005. "A Millennial Scale Planktonic Foraminifer Record of the Mid-Pleistocene Climate Transition from the Northern South China Sea." *Palaeogeography, Palaeoclimatology, Palaeoecology* 223, 349–63.

REFERÊNCIAS

ANDREASEN, D.J.; RAVELO, A.C. Tropical Pacific Ocean thermocline reconstructions for the last glacial maximum. *Paleoceanography*, v. 12, p. 395–413, 1997.

BÉ, A.W.H. Foraminifera, families: Globigerinidae and Globor- otaliidae. In: Fraser, J.H. (Ed.), Fiches d'Indentification du Zooplancton,Cons. Int.Explor.Mer,Charlottenlund, Sheet, 1967.

CHAPORI, N.G.; CHIESSI, C.M.; BICKERT, T.; LAPRIDA, C. Sea-surface temperature reconstruction of the Quaternary Western South Atlantic: New planktonic foraminiferal correlation function. *Palaeogeography, Palaeoclimatology, Palaeoecology*, v. 425, p. 67-75, 2015.

CHEN, C.; JAN, S.; KUO, T.; LI, S. Nutrient flux and transport by the Kuroshio east of Taiwan. *Journal of Marine Systems*, v. 167, p. 43–54, 2017.

CHEN, M.-T.; HUANG, C.C.; PFLAUMANN, U.; WAELBROECK, C.; KUCERA, M. Estimating Glacial Western Pacific Sea-Surface Temperature: Methodological Overview and Data Compilation of Surface Sediment Planktic Foraminifer Faunas. *Quaternary Science Reviews*, v. 24, p. 1049–62, 2005.

CHEN, M.-T.; HO, H.-W.; LAI, T.-D.; ZHENG, L.; MIAO, Q.; SHEA, K.-S.; … HUANG, C.-Y. Recent planktonic foraminifers and their relationships to surface ocean hydrography of the South China Sea. *Marine Geology*, v. 146, p. 173–190, 1998.

CHEN, M.-T.; SHIAU, L.-J.; YU, P.-S.; CHIU, T.-C.; CHEN, Y.-G.; WEI, K.-Y. 500 000-Year records of carbonate, organic carbon, and foraminiferal sea-surface temperature from the southeastern South China Sea (near Palawan Island). *Palaeogeography, Palaeoclimatology, Palaeoecology*, v. 197, p. 113–131, 2003.

CHEN, M.-T.; WANG, P.; WANG, L.; SARNTHEIN, M.; WANG, C.H.; HUANG, C.Y. A late Quaternary planktonic foraminifer faunal record of rapid climatic changes from the South China Sea. *Marine Geology*, v. 156, p. 85–108, 1999.

CHEN, M.-T.A.; WANG, S.-L.; CHOU, W.-C.; SHEU, D.D. Carbonate chemistry and projected future changes in pH and CaCO3 saturation state of the South China Sea. *Marine Chemistry*, v. 101, p. 277–305, 2006.

CHENG, H.; SINHA, A.; WANG, X.; CRUZ, F.W.; EDWARDS, R.L. The Global Paleomonsoon as seen through speleothem records from Asian and the Americas. *Climate Dynamics*, v. 39, p. 1045–1062, 2012.

CHENG, X.; HUANG, B.; JIAN, Z.; ZHAO, Q.; TIAN, J.; LI, J. Foraminiferal isotopic evidence for monsoonal activity in the South China Sea: A present-LGM comparison. *Marine Micropaleontology*, v. 54, p. 125–139, 2005.

CLEMENS, S.C.; PRELL, W.L.; SUN, Y. Orbital-scale timing and mechanisms driving Late Pleistocene Indo-Asian summer monsoons: Reinterpreting cave speleothem D18O. *Paleoceanography*, v. 25, p. 1–19, 2010.

DE GARIDEL-THORON, T., BEAUFORT, L., LINSLEY, B. K.; DANNENMANN, S. Millennial-scale dynamics of the East Asian winter monsoon during the last 200,000 years. *Paleoceanography*, v. 16, p. 491–502, 2001.

DONG, L., LI, L., LI, Q., WANG, H.; ZHANG, C. L. Hydroclimate implications of thermocline variability in the southern South China Sea over the past 180,000yr. *Quaternary Research* (United States), v. 83, p. 370–377, 2015.

DONGHUAI, S. Monsoon and westerly circulation changes recorded in the late Cenozoic aeolian sequences of Northern China. *Global and Planetary Change*, v. 41, p. 63–80, 2004.

DUAN, R.; YANG, K.; MA, Y.; HU, T. A Study of the Mixed Layer of the South China Sea Based on the Multiple Linear Regression. *Acta Oceanologica Sinica*, v. 31, p. 19–31, 2012.

FAIRBANKS, R.G.; SVERDLOVE, M.; FREE, R.; WIEBE, P.H.; BÉ, A.W.H. Vertical distribution and isotopic fractionation of living planktonic foraminifera from the Panama Basin. *Nature*, v. 298, p. 841–844, 1982.

FERREIRA, P.A.L.; COSTA, K.B.; TOLEDO, F.A.L.; FIGUEIRA, R.C.L. Sedimentation rates and age modeling of Late Quaternaty marine sediments with unsupported 230Th. *Journal of Radioanalytical and Nuclear Chemistry*, v. 304, p. 829-836, 2015.

GROOTES, P. M.; STUIVER, M. Oxygen 18/16 variability in Greenland snow and ice with 10 -3- to 105-year time resolution. *Journal Of Geophysical Research*, v. 102, p. 455-470, 1997.

GUIOT, J.; DE VERNAL, A. Transfer functions: methods for qualitative paleoceanography based on microfossils. In: C. Hillarie-Marcel & A. De Vernal (eds.). Proxies in Late Cenozoic Paleoceanography, v. 1, p. 523–563, 2007.

GUO, X.; ZHU, X.; WU, Q.; HUANG, D. The Kuroshio nutrient stream and its temporal variation in the East China Sea. *Journal of Geophysical Research*, v. 117, p. 1-17, 2012.

GUO, Z.T.; BERGER, A.; YIN, Q.Z.; QIN, L. Strong asymmetry of hemispheric climates during MIS-13 inferred from correlating China loess and Antarctica ice records. *Climate of the Past Discussions*, v. *5*, p. 21-31, 2008.

GUPTA, A.K.; ANDERSON, D.M.; OVERPECK, J.T. Abrupt changes in the Asian southwest monsoon during the Holocene and their links to the North Atlantic Ocean. *Nature*, v. 421, p. 4–7, 2003.

HAMMER, O.; Harper, D.A.T.; Rian, P.D. *Past. Palaeonthological statistics software package for education and data analysis.* Version. 2.17, 2001.

HE, J.; ZHAO, M.; WANG, P.; LI, L.; LI, Q. Changes in phytoplankton productivity and community structure in the northern South China Sea during the past 260 ka. *Palaeogeography, Palaeoclimatology, Palaeoecology*, v. 392, p. 312–323, 2013.

HE, Z.; WU, R. Coupled seasonal variability in the South China Sea. Journal of Oceanography, v. 69, n. 1, p. 57–69, 2013.

HEMLEBEN, C.; SPINDLER, M.; ANDERSON, O.R. *Modern Planktonic Foraminifera*. Springer, New York, 1989.

HESS, S.; KUHNT, W. Neogene and Quaternary paleoceanographic changes in the southern South China Sea (Site 1143): The benthic foraminiferal record. *Marine Micropaleontology*, v. 54, n. 1-2, p. 63–87, 2005.

JIAN, Z.; HUANG, B.; KUHNT, W.; LIN, H.-L. Late Quaternary Upwelling Intensity and East Asian Monsoon Forcing in the South China Sea. *Quaternary Research*, v. 55, n. 3, p. 363–370, 2001.

JIAN, Z., LI, B., HUANG, B.; WANG, J. Globorotalia truncatulinoides as indicator of upper-ocean thermal structure during the Quaternary: Evidence from the South China Sea and Okinawa Trough. *Palaeogeography, Palaeoclimatology, Palaeoecology*, v. 162, n. 3-4, p. 287–298, 2000.

JONKERS, L.; KUČERA, M. Global analysis of seasonality in the shell flux of extant planktonic Foraminifera. *Biogeosciences*, v. 12, n. 7, p. 2207–2226, 2015.

KAO, S.J.; WU, C.; HSIN, Y.; DAI, M. Effects of sea level change on the upstream Kuroshio Current through the Okinawa Trough. *Geophysical Research Letters*, v. 33, p. 1–5, 2006.

KELLER, G. Depth stratification of planktonic foraminifers in the Miocene ocean. In Kennett, J.P. (Ed.), The Miocene Ocean: *Paleoceanography and Biogeography*. *Geologycal Society of America*, v. 163, p. 177-196, 1985.

KIENAST, M. Synchronous Tropical South China Sea SST Change and Greenland Warming During Deglaciation. *Science*, v. 291, n. 5511, p. 2132–2134, 2001.

KIENAST, M.; STEINKE, S.; STATTEGGER, K.; CALVERT, S.E. Synchronous Tropical South China Sea SST Change and Greenland Warming During Deglaciation. *Science*, v. 291, p. 2132-2134, 2001.

KUCERA, M. *Chapter Six Planktonic Foraminifera as Tracers of Past Oceanic Environments*. v. 1, p. 213–262, 2007.

KUCERA, M.; WEINELT, M.; KIEFER, T.; PFLAUMANN, U.; HAYES, A.; WEINELT, M.; CHEN, M-T.; MIX, A.C.; BARROWS, T.T.; CORTIJO, E.; DUPRAT, J.; JUGGINS, S.; WAELBROECK, C. Reconstruction of sea-surface temperatures from assemblages of planktonic foraminifera: Multi-technique approach based on geographically constrained calibration data sets and its application to glacial Atlantic and Pacific Oceans. *Quaternary Science Reviews*, v. 24, SPEC. ISS., p. 951–998, 2005.

KUROYANAGI, A.; KAWAHATA, H. Vertical distribution of living planktonic foraminifera in the seas around Japan. *Marine Micropaleontology*, v. 53, n. 1-2, 173–196, 2004.

LANG, N.; WOLFF, E.W. Interglacial and glacial variability from the last 800 ka in marine, ice and terrestrial archives. *Climate of the Past*, v. 7, p. 361–380, 2011.

LI, B.; JIAN, Z.; LI, Q.; TIAN, J.; WANG, P. Paleoceanography of the South China Sea since the middle Miocene: Evidence from planktonic foraminifera. Marine Micropaleontology, v. 54, p. 49–62, 2005.

LI, B.; WANG, J.; HUANG, B.; LI, Q.; JIAN, Z.; ZHAO, Q.; SU, X.; WANG P. Correction to "South China Sea surface water evolution over the last 12 Myr: A south-north comparison from Ocean Drilling Program Sites 1143 and 1146." *Paleoceanography*, v. 19, n. 1, p. 1–12, 2004.

LI, C.-F.; LIN, J.; KULHANEK, D.K.; WILLIAMS, T.; BAO, R.; BRIAIS, A.;… ZHAO, X. 2015. Site U1431. In Li, C.-F., Lin, J., Kulhanek, D.K. and the Expedition 349 Scientists, *Proceedings of the International Ocean Discovery Program, 349: South China Sea Tectonics: College Station, TX (International Ocean Discovery Program)*, 2015.

LI, C.-F.; XU, X.; LIN, J.; SUN, Z.; ZHU, J.; YAO, Y.;… ZHANG, G.-L. Ages and magnetic structures of the South China Sea constrained by deep tow magnetic surveys and IODP Expedition 349. *Geochemistry, Geophysics, Geosystems*, v. 15, n. 12, p. 4958–4983, 2014.

LI, D.; CHIANG, T.; KAO, S.; HSIN, Y.; ZHENG, L.; YANG, J.T.; … DAI, M. Journal of Asian Earth Sciences Circulation and oxygenation of the glacial South China Sea. *Journal of Asian Earth Sciences*, v. 138, p. 387–398, 2017.

LI, Q.; WANG, P.; ZHAO, Q.; TIAN, J.; CHENG, X.; JIAN, Z.; ZHONG, G.; CHEN, M. Paleoceanography of the mid-Pleistocene South China Sea. *Quaternary Science Reviews*, v. 27, p. 1217–1233, 2008.

LI, T., ZHAO, J., SUN, R., CHANG, F.; SUN, H. Marine Micropaleontology The variation of upper ocean structure and paleoproductivity in the Kuroshio source region during the last 200 kyr. *Marine Micropaleontology*, v. 75, n. 1-4, p. 50–61, 2010.

LIN, H.-L.; HSIEH, H.-Y. Seasonal variations of modern planktonic foraminifera in the South China Sea. *Deep Sea Research Part II: Topical Studies in Oceanography*, v. 54, n. 14-15, p. 1634–1644, 2007.

LISIECKI, L.E.; RAYMO, M.E. A Pliocene-Pleistocene stack of 57 globally distributed benthic δ 18 O records. *Paleoceanography*, v. 20, n. 1, 2005.

LIU, G.; CHAI, F. Seasonal and interannual variability of primary and export production in the South China Sea : a three-dimensional physical – biogeochemical model study, *International Council for the Exploration of the Sea*, p. 420–431, 2009.

LIU, J.; LI, T.; XIANG, R.; CHEN, M.; YAN, W.; CHEN, Z.; LIU, F. Influence of the Kuroshio Current intrusion on Holocene environmental transformation in the South China Sea. *The Holocene*, v. 23, p. 850-859, 2013.

LIU, K.; CHAO, S.; SHAW, P.; GONG, G.; CHEN, C.; TANG, T.Y. Monsoon-forced chlorophyll distribution and primary production in the South China Sea : observations and a numerical study. *Deep-Sea Research*, v. 49, p. 1387–1412, 2002.

LIU, Q.; JIANG, X.; XIE, S. P.; LIU, W. T. A gap in the Indo-Pacific warm pool over the South China Sea in boreal winter: Seasonal development and interannual variability. *Journal of Geophysical Research C: Oceans*, v. 109, n. 16, p. 1–10, 2004.

LIU, Q.; KANEKO, A.; SU, J. Recent progress in studies of the South China Sea circulation. *Journal of Oceanography*, v. 64, n. 5, p. 753–762, 2008.

LIU, Z.; COLIN, C.; LI, X.; ZHAO, Y.; TUO, S.; CHEN, Z.;…HUANG, K.-F. Clay mineral distribution in surface sediments of the northeastern South China Sea and surrounding fluvial drainage basins: Source and transport. *Marine Geology*, v. 277, n. 1-4, p. 48–60, 2010.

LIU, Z.; ZHAO, Y.; COLIN, C.; STATTEGGER, K.; WIESNER, M. G.; HUH, C.-A.;…Li, Y. Source-to-Sink transport processes of fluvial sediments in the South China Sea. *Earth-Science Reviews*,v. 153, p. 238-273, 2015.

MARGO. *MARGO Multiproxy Approach for the Reconstruction of the Glacial Ocean surface* (archived project web pages and templates), Bremerhaven, PANGAEA, 2004.

MCCLYMONT, E.L.; SOSDIAN, S.M.; ROSELL-MELÉ, A.; ROSENTHAL, Y. Pleistocene sea-surface temperature evolution: Early cooling, delayed glacial intensification, and implications for the mid-Pleistocene climate transition. Earth-Science Reviews, v. 123, p. 173–193, 2013.

MOREY, A.E.; MIX, A.C.; PISIAS, N.G. Planktonic foraminiferal assemblages preserved in surface sediments correspond to multiple environment variables. Quaternary Science Reviews, v. 24, p. 925-950, 2005.

NATHAN, S.A.; LECKIE, R. Miocene planktonic foaminiferal biostratigraphy of Sites 1143 and 1146, ODP Leg 184, South China Sea. In: Prell, WL; Wang, P; Blum, P; Rea, DK; Clemens, SC (eds.) *Proceedings of the Ocean Drilling Program*, Scientific Results, College Station, TX (Ocean Drilling Program), v. 184, p. 1-43, 2003.

OPPO, D.W.; SUN, Y. Amplitude and timing of sea-surface temperature change in the northern South China Sea : Dynamic link to the East Asian monsoon. *Geological Society of America*, v. 33, n. 10, p. 785-788, 2005.

PAILLARD, D., LABEYRIE, L.; YIOU, P. AnalySeries 1.0: a Macintosh software for the analysis of geophysical time-series. *Eos Transactions, AGU*, v. 77, pp. 379, 1996.

PARKER, F.L. Planktonic foraminiferal species in Pacific sediments. *Micropaleontology*, v. 8, n. 2, p. 219-254, 1962.

PARKER, W.C.; ARNOLD, A.J. *Quantitative methods of data analysis in foraminiferal ecology*. In: Gupta, B.K.S. Modern Foraminifera. Published by Kluwer Academic Publishers, Grain Bretain. pp 71-89, 1999.

PEETERS, F.J.C., BRUMMER, G.-J.A.; GANSSEN, G.M. The effect of upwelling on the distribution and stable isotope composition of Globigerina bulloides and Globigerinoides ruber (planktic foraminifera) in modern surface waters of the NW Arabian Sea. *Global and Planetary Change*, v. 34, p. 269–291, 2002.

PFLAUMANN, U.; JIAN, Z. Modern distribution patterns of planktonic foraminifera in the South China Sea and western Pacific : a new transfer technique to estimate regional sea-surface temperatures. *Marine Geology*, v. *156, n.* 1-4, p. 41–83, 1999.

PRELL, W.L.; CURRY, W.B. Faunal and isotope indices of monsoonal upwelling: Western Arabia Sea. *Oceanologica Acta*, v. 4, p. 91–98, 1981.

QU, T. Role of ocean dynamics in determining the mean seasonal cycle of the South China Sea surface temperature. *Journal of Geophysical Research*, v. 106, n. C4, p. 6943–6955, 2001.

REGENBERG, M.; REGENBERG, A.; GARBE-SCHÖNBERG, D.; LEA, D.W. Global dissolution effects on planktonic foraminiferal Mg/Ca ratios controlled by the calcite-saturation state of bottom waters. *Paleoceanography*, v. 29, n. 3, p. 127–142, 2014.

REIMER, P.J.; BARD, E.; BAYLISS, A.; BECK, J.W.; BLACKWELL, P.G.; RAMSEY, C.B. IntCal13 and Marine13 Radiocarbon Age Calibration Curves 0–50,000 Years cal BP. *Radiocarbon*, v. 55, n. 4, p. 1869–1887, 2013.

REN, H.; SIGMAN, D.M.; CHEN, M.; KAO, S. Elevated foraminifera-bound nitrogen isotopic composition during the last ice age in the South China Sea and its global and regional implications. *Global Biogeochemical Cycles*, v. 26, p. 1–13, 2012.

SALMON, K. H.; ANAND, P.; SEXTON, P.F.; CONTE, M. Upper ocean mixing controls the seasonality of planktonic foraminifer fluxes and associated strength of the carbonate pump in the oligotrophic North Atlantic. *Biogeosciences*, v. 12, n. 1, p. 223–235, 2015.

SCHIEBEL, R. Planktic foraminiferal sedimentation and the marine calcite budget. *Global Biogeochemical Cycles*, v. *16, n.* 4, p. 3-1-3-21, 2002.

SCHIEBEL, R.; HEMLEBEN. *Planktic Foraminifers in the Modern Ocean: Ecology, Biogeochemistry, and Application*. Springer. ISBN 3662502976, 9783662502976, pp. 333, 2016.

SCHIEBEL, R.; ZELTNER, A.; TREPPKE, U.F.; WANIEK, J.J.; BOLLMANN, J.; RIXEN, T.; HEMLEBEN, C. Distribution of diatoms, coccolithophores and planktic foraminifers along a trophic gradient during SW monsoon in the Arabian Sea. *Marine Micropaleontology*, v. 51, p. 345–371, 2004.

SHI, X.; WU, Y.; ZOU, J.; LIU, Y.; GE, S.; ZHAO, M.;…HAN, Y. Multiproxy reconstruction for Kuroshio responses to northern hemispheric oceanic climate and the Asian Monsoon since Marine. *Climate of the Past*, v. 10, p. 1735–1750, 2014.

SHYU, J-P; CHEN, M-P; SHIEH, Y-T; HUANG, C-K. A Pleistocene paleoceanographic record from the north slope of the Spratly Islands , southern South China Sea. *Marine Micropaleontology*, v. 42, p. 61-93, 2001.

SISWANTO, E., YE, H., YAMAZAKI, D.; TANG, D.L. Detailed spatiotemporal impacts of El Niño on phytoplankton biomass in the South China Sea. *Journal of Geophysical Research: Oceans*, v. 122, n. 4, p. 1-15, 2017.

STEINKE, S.; CHIU, H.Y.; YU, P-S.; SHEN, C.C.; ERLENKEUSER, H.; LÖWEMARK., L.; CHEN, M.T. "On the Influence of Sea Level and Monsoon Climate on the Southern South China Sea Freshwater Budget over the Last 22,000 Years." *Quaternary Science Reviews*, v. 25, p. 1475–88, 2006.

STEINKE, S.; GLATZ, C.; MOHTADI, M.; GROENEVELD, J.; LI, Q.; JIAN, Z. Past dynamics of the East Asian monsoon: No inverse behaviour between the summer and winter monsoon during the Holocene. *Global and Planetary Change*, v. 78, n. 3-4, p. 170-177, 2011.

STEINKE, S.; KIENAST, M.; PFLAUMANN, U.; WEINELT, M.; STATTEGGER, K. A High-Resolution Sea-Surface Temperature Record from the Tropical South China Sea (16,500–3000 Yr B.P.). *Quaternary Research*, v. 55, n. 3, p. 352–62, 2001.

STEINKE, S.; MOHTADI, M.; GROENEVELD, J.; LIN, L.C.; LÖWEMARK., L; CHEN, M.T.; RENDLE-BÜHRING, R. Reconstructing the Southern South China Sea

Upper Water Column Structure since the Last Glacial Maximum : Implications for the East Asian Winter Monsoon Development. *Paleoceanography*, v. 25, p. 1–15, 2010.

STEINKE, S.; YU, P-S.; KUCERA, M.; CHEN, M-T. No-analog planktonic foraminiferal faunas in the glacial southern South China Sea: Implications for the magnitude of glacial cooling in the western Pacific warm pool. *Marine Micropaleontology*, v. 66, p. 71-90, 2008.

SU, X.; LIU, C.; BEAUFORT, L.; BARBARIN, N.; JIAN, Z. Differences in Late Quaternary primary productivity between the western tropical Pacific and the South China Sea: Evidence from coccoliths. *Deep-Sea Research Part II: Topical Studies in Oceanography*, v. 122, p. 131–141, 2015.

SU, X.; LIU, C.; BEAUFORT, L.; TIAN, J.; HUANG, E. Late Quaternary coccolith records in the South China Sea and East Asian monsoon dynamics. *Global and Planetary Change*, v. 111, p. 88–96, 2013.

SUN, Y.; CLEMENS, S.C.; MORRILL, C.; LIN, X.; WANG, X.; AN, Z. Influence of Atlantic meridional overturning circulation on the East Asian winter monsoon. *Nature Geoscience*, v. 5, n. 1, p. 46–49, 2011.

TIAN, J.; HUANG, E.; PAK, D. East Asian winter monsoon variability over the last glacial cycle: insights from a latitudinal sea-surface temperature gradient across the South China Sea. *Palaeogeography, Palaeoclimatology, Palaeoecology*, v. 292, p. 319–324, 2010.

TIAN, J.; WANG, P.X.; CHEN, R.H.; CHENG, X.R. Quaternary upper ocean thermal gradient variations in the South China Sea: Implications for east Asian monsoon climate. *Paleoceanography*, v. 20, n. 4, p. 1-8, 2005.

Venegas, S. A. *Statistical Methods for Signal Detection in Climate*. University of Copenhagen, Copenhagen, Denmark, 96 pp, 2001.

WAN, S.M.; LI, A.C.; CLIFT, P. D.; WU, S.G.; XU, K.H.; LI, T.G. Increased contribution of terrigenous supply from Taiwan to the northern South China Sea since 3 Ma. *Marine Geology*, v. 278, p. 115–121, 2010.

WANG, B.; DING, Q. Global monsoon: dominant mode of annual variation in the tropics. *Dynamics of Atmospheres and Oceans*, v. 44, p. 165–183, 2008.

WANG, L.; SARNTHEIN, M.; ERLENKEUSER, H.; GRIMALT, J.O.; GROOTES, P.; HEILIG, S.; IVANOVA, E.; KIENAST, M.; PELEJERO, C.; PFLAUMANN, U. East Asian monsoon climate during the latePleistocene: High-resolution sediment records from the South China Sea. *Marine Geology*, v. 156, p. 243–282, 1999.

WANG, L.; WANG, P. Late Quaternary paleoceanography of the South China Sea: glacial=interglacial contrasts in an enclosed basin. *Paleoceanography*, v. 5, p. 77–90, 1990.

WANG, P.; Q. LI. *Oceanographical and geological background, in The South China Sea, Development in Paleoenvironmental Research*, vol. 13, edited by P. Wang and Q. Li, Springer Science+Business Media B.V., Netherlands, pp. 73, 2009.

WANG, P.; CLEMENS, S.; BEAUFORT, L.; BRACONNOT, P.; GANSSEN, G.; JIAN, Z.;…SARNTHEIN, M. Evolution and variability of the Asian monsoon system: state of the art and outstanding issues. *Quaternary Science Reviews*, v. 24, n. 5-6, p. 595–629, 2005.

WANG, P.; LI, Q.; TIAN, J. Pleistocene paleoceanography of the South China Sea: Progress over the past 20 years. *Marine Geology*, v. 352, p. 381–396, 2014.

WANG, P.; WANG, L.; BIAN, Y.; JIAN, Z. Late Quaternary paleoceanography of the South China Sea: surface circulation and carbonate cycles. *Marine Geology*, v. 127, n. 1–4, p. 145–165, 1995.

WANG, R. J.; JIAN, Z.M.; XIAO, W.S.; TIAN, J.; LI, J.R.; CHEN, R.H.; ZHENG, Y.L.; CHEN, J.F. Quaternary biogenic opal records in the South China Sea: Linkages to East Asian monsoon, global ice volume and orbital forcing. *Science in China Series D: Earth Sciences*, v. 50, p. 710–724, 2007.

WANG, Y.; CHENG, H.; EDWARDS, R.L.; KONG, X.; SHAO, X.; CHEN, S.; … AN, Z. Millennial- and orbital-scale changes in the East Asian monsoon over the past 224,000 years. *Nature*, v. 451, n. 7182, p. 1090–1093, 2008a.

WANG, Y.; CHENG, H.; EDWARDS, R. L.; HE, Y.; KONG, X.; AN, Z.; WU, J.; KELLY, M. J.; DYKOSKI, C. A.; LI, X. The Holocene Asian monsoon: links to solar changes and North Atlantic climate. Science (New York, N.Y.), v. 308, n. 5723, p. 854–857, 2005b.

WEFER, G.; BERGER, W.H.; BIJMA, J.; FISCHER, G. Clues to Ocean History: a brief overview of proxies. In: Fischer, G.; Wefer, G. (eds.). *Use of Proxies in Paleoceanography - Examples from the South Atlantic*. Berlin Heidelberg: Springer, p. 1-68, 1999.

WEI, G.; DENG, W.; LIU, Y.; LI, X. High-resolution sea surface temperature records derived from foraminiferal Mg / Ca ratios during the last 260 ka in the northern South China Sea. *Palaeogeography, Palaeoclimatology, Palaeoecology*, v. 250, p. 126–138, 2007.

WEI, K., CHIU, T.; CHEN, Y. Toward establishing a maritime proxy record of the East Asian summer monsoons for the late Quaternary. *Marine Geology,* v. 201, p. 67–79, 2003.

XIANJUN, X.; DONGXIAO, W.; WEN, Z.; ZUQIANG, Z.; YINGHAO, Q.I.N.; NA, H.E.; LILI, Z. Impacts of a wind stress and a buoyancy flux on the seasonal variation of mixing layer depth in the South China Sea. *Acta Oceanologica Sinica,* v. 32, n. 9, p. 30–37, 2013.

XU, J.; WANG, P.; HUANG, B.; LI, Q.; JIAN, Z. Response of planktonic foraminifera to glacial cycles: Mid-Pleistocene change in the southern South China Sea. *Marine Micropaleontology*, v. 54, p. 89–105, 2005.

XUE, H. J.; CHAI, F.; PETTIGREW, N.; XU, D.Y.; SHI, M.; XU, J. P. Kuroshio intrusion and the circulation in the South China Sea. *Journal of Geophysical Research-Oceans,* v. 109, n. C2, 2004.

YANASE, W.; OUCHI, A. The LGM surface climate and atmospheric circulation over East Asia and the North Pacific in the PMIP2 coupled model simulations. *Climate of the Past,* v. 3, p. 439–451, 2007.

YU, G.; CHEN, X.; NI, J.; CHEDDADI, R.; GUIOT, J.; HAN, H.;…;HUANG, C. Palaeovegetation of China : a pollen data-based synthesis for the mid-Holocene and last glacial maximum. *Journal of Biogeography*, v. 27, n. 3, p. 635–664, 2000.

YU, P-S.; CHEN, M. Millennial-to-orbital scale changes in the planktic foraminiferal assemblages and sea surface temperature in the South China Sea during the Past 135 Kya. *Geophysical Research Abstracts*, v. 15, p. 9190, 2013.

YU, P.-S.; HUANG, C.-C.; CHIN, Y.; MII, H.-S.; CHEN, M.-T. Late Quaternary East Asian Monsoon variability in the South China Sea: evidence from planktonic foraminifera faunal and hydro- graphic gradient records. *Palaeogeography, Palaeoclimatology, Palaeoecology*, v. 236, n. 1-4, p. 74-90, 2006.

YU, P-S.; MII, H. S.; MURAYAMA, M.; CHEN, M-T. Late Quaternary Planktic Foraminifer Fauna and Monsoon Upwelling Records from the Western South China Sea, near the Vietnam Margin (IMAGES MD012394). *Terrestrial, Atmospheric and Oceanic Sciences*, v. 19, p. 347–62, 2008.

ZARIC, S.; DONNER, B.; FISCHER, G.; MULITZA, S.; WEFER, G. Sensitivity of planktic foraminifera to sea surface temperature and export production as derived from sediment trap data. *Marine Micropaleontology,* v. 55, n. 1-2, p. 75–105, 2005.

ZARIC, S.; SCHULZ, M.; MULITZA, S. Global prediction of planktonic foraminiferal fluxes from hydrographic and productivity data. *Biogeosciences,* v. 55, p. 77-105, 2005.

ZHANG, L., CHEN, M., XIANG, R., ZHANG, L.; LU, J. Marine Micropaleontology Productivity and continental denudation history from the South China Sea since the late Miocene. *Marine Micropaleontology*, v. 72, n. 1-2, p. 76–85, 2009.

ZHANG, P. Z.; CHENG, H.; EDWARDS R.L.; CHEN F.H.; WANG Y.J.; YANG X.L.; LIU, J.; TAN, M.; WANG, X.F.; LIU, J.H.; AN, C.L.; DAI, Z.B.; ZHOU, J.; ZHANG,

D.Z; JIA, J.H.; JIN, L.Y.; JOHNSON, K.R. A test of climate, sun, and culture relationships from a 1810-year Chinese Cave record. *Science*, v. 322, p. 940-942, 2008.

ZHENG, F.; LI, Q.; LI, B.; CHEN, M.; TU, X.; TIAN, J.; JIAN, Z. A millennial scale planktonic foraminifer record of the mid-Pleistocene climate transition from the northern South China Sea. *Palaeogeography, Palaeoclimatology, Palaeoecology*, v. 223, p. 349-363, 2005.